Supporting information for

Re(I)-quinolinate-pyridyl complexes with free disubstituted benzimidazole pharmacophore as anticancer agents

Reema L. Borkar, Chandra Lekha Putta, Merlin Platto, Nitisha Beniwal, Bharati Banoth, Abhishesh Kumar Mehata, Shanmugam Ramasamy, Aravind Kumar Rengan

Contents

Fig. S26 (A) Detection of DNA damage after being treated with **Re-F** and cisplatin. Control (Untreated 4T1 cells) was used as a negative control and cells treated with cisplatin were used as a positive control (Scale bar: 20 μm). (B) Quantification data of fluorescence intensity.

Table S1-S2 Crystal data and structure refinement for the complexes
Table S3 Selected bond lengths [Å] for the complexes.

Supporting Information for Computational Theory Selection

Table S4 Bond distance, average bond distance, and difference of calculated bond distance from the experiment. All the values reported here are in Å.

Supporting Information for molecular docking studies

Table S5 Metal complexes binding energy [kcal/mol] with various DNA models

Supporting Information for molecular dynamics simulations

Fig. S27 Time evoluation of RMSD of metal complexes-1Z3F A) **Re-F**, B) **Re-Cl**, C) **Re-Br**, D) **Re-Me**, and E) **Re-Np**. The metal complexes are colored in blue for better visualization in the 3D representation. The inserted snapshot in the plot is taken at 0 ns, 300 ns, and 600 ns respectively. The atoms' colors are represented as follows: Grey – C, Black – H, Blue – N, Red – O, Cyan – Re, Pale blue – F, Green – Cl , and Brown – Br.

Table S6 MMPBSA calculations of **Re-F**, **Re-Cl**, **Re-Br**, **Re-Me,** and **Re-Np** with 1Z3F. All values are reported in kcal/mol.

Synthesis of Ligands

Synthesis of L-F

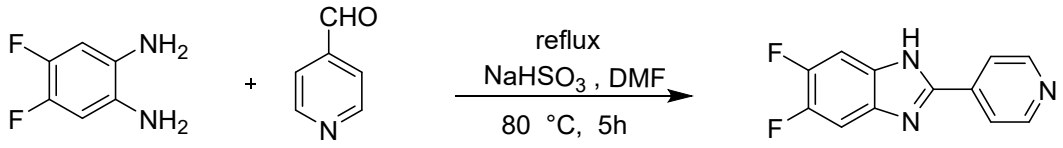

A mixture of 4,5-difluorobenzene-1,2-diamine (200 mg, 1.39 mmol) and $NaHSO_3$ (577 mg, 5.55 mmol) was added to the round-bottom flask. To this mixture, DMF (6 mL) and then 4-pyridinecarboxyaldehyde (148 mg, 1.38 mmol) were added. The reaction mixture was allowed to stir at 80 ℃ for 5 hours. The progress of the reaction was monitored by thin-layer chromatography (TLC). After completion, the reaction mixture was poured into ice-cold water, filtered, and a light brown powder was obtained. Yield: 56 % (180 mg).

Synthesis of L-Cl

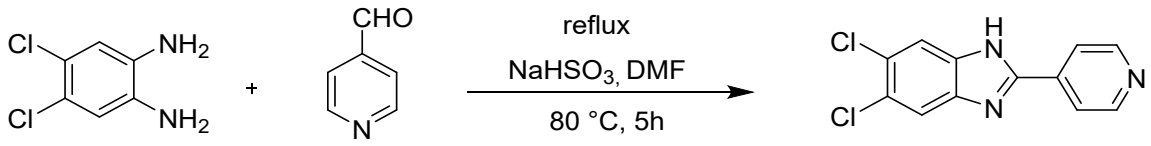

By following the procedure similar to L-F, L-Cl was obtained using a mixture of 4,5-dichlorobenzene-1,2-diamine (201 mg, 1.13 mmol), $NaHSO_3$ (312 mg, 3.01 mmol), 4-pyridinecarboxyaldehyde (120 mg, 1.13 mmol) and DMF (6 mL). After completion, the reaction mixture was poured into ice-cold water, filtered, and a light brown powder was obtained. Yield: 98 % (225 mg).

Synthesis of L-Br

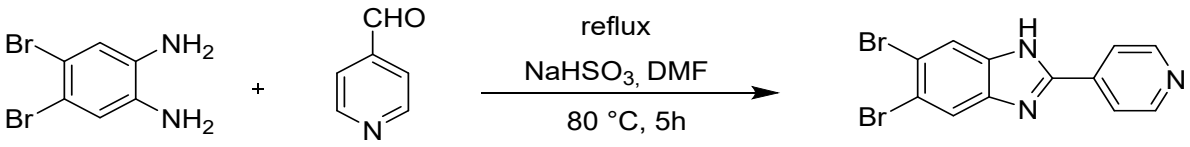

By following the procedure similar to L-F, L-Br was obtained using a mixture of 4,5-dibromobenzene-1,2-diamine (200 mg, 0.75 mmol), $NaHSO_3$ (312 mg, 3.01 mmol), 4-pyridinecarboxyaldehyde (121 mg, 1.13 mmol) and DMF (6 mL). After completion, the reaction mixture was poured into ice-cold water, filtered, and a light brown powder was obtained. Yield: 69 % (184 mg).

Synthesis of L-Me

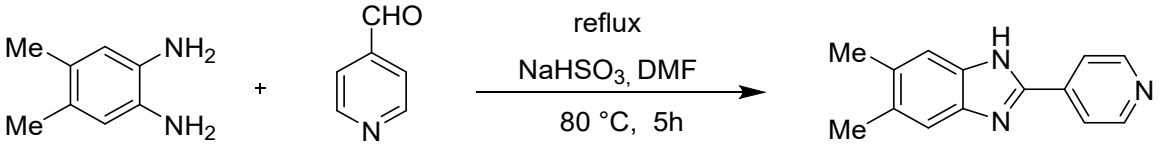

By following the procedure similar to L-F, L-Me was obtained using a mixture of 4,5-dimethylbenzene-1,2-diamine (202 mg, 1.48 mmol), $NaHSO_3$ (611 mg, 5.87 mmol), 4-pyridinecarboxyaldehyde (157 mg, 1.47 mmol) and DMF (6 mL). After completion, the reaction mixture was poured into ice-cold water, filtered, and a light brown powder was obtained. Yield: 56 % (182 mg).

Synthesis of L-Np

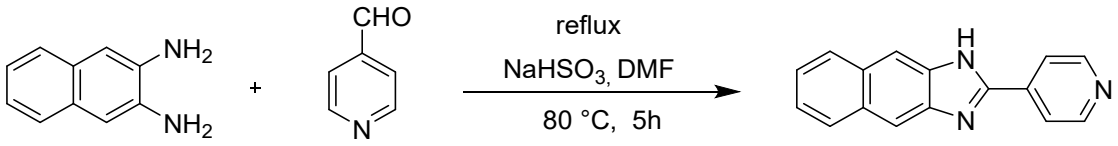

By following the procedure similar to L-F, L-Np was obtained using a mixture of naphthalene-2,3-diamine (202 mg, 1.26 mmol), $NaHSO_3$ (526 mg, 5.06 mmol), 4-pyridinecarboxyaldehyde (135 mg, 1.26 mmol) and DMF (6 mL). After completion, the reaction mixture was poured into ice-cold water, filtered, and a light brown powder was obtained. Yield: 57 % (178 mg).

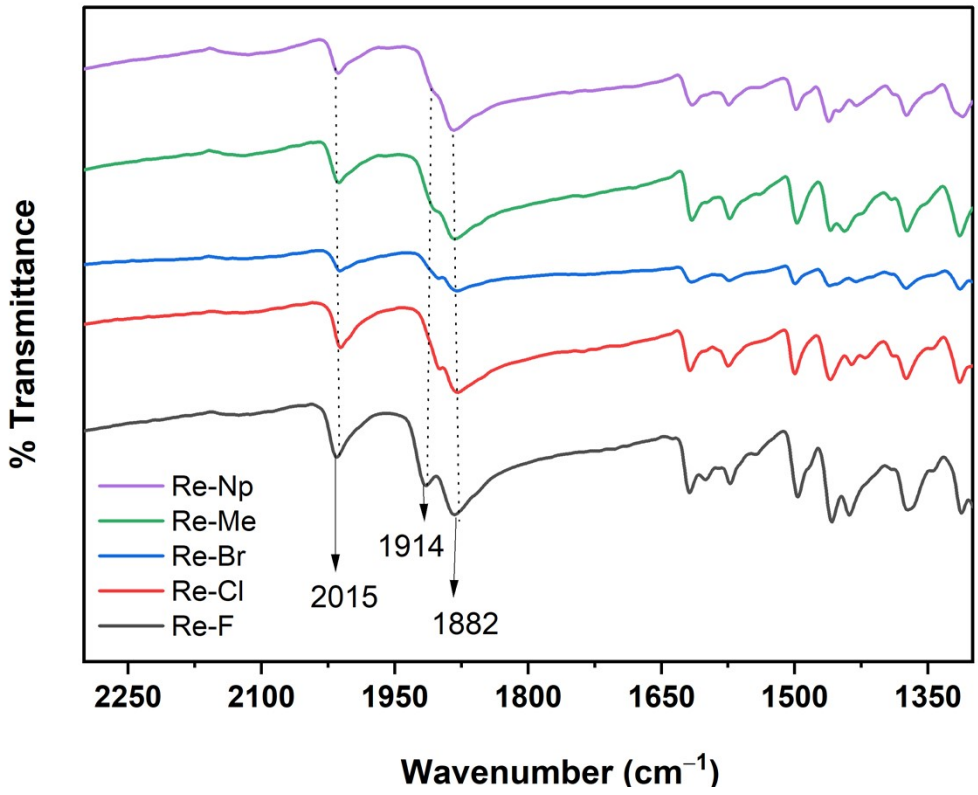

Fig. S1 ATR-IR spectra of **Re-F**, **Re-Cl**, **Re-Br**, **Re-Me** and **Re-Np**.

Analysis Info

Analysis Name	F:\HRMS_ACYCLIC\raw\RB4-296.d	Acquisition Date	22-11-2024 11:32:31
Method	DEFAULT.m	Operator	UOH
Sample Name	RB4-296	Instrument	maXis 255552.10138
Comment			

Acquisition Parameter

Source Type	ESI	Ion Polarity	Positive	Set Nebulizer	0.5 Bar
Focus	Not active	Set Capillary	3000 V	Set Dry Heater	200 C
Scan Begin	50 m/z	Set End Plate Offset	-500 V	Set Dry Gas	4.0 l/min
Scan End	1600 m/z	Set Charging Voltage	2000 V	Set Divert Valve	Waste
		Set Corona	0 nA	Set APCI Heater	0 C

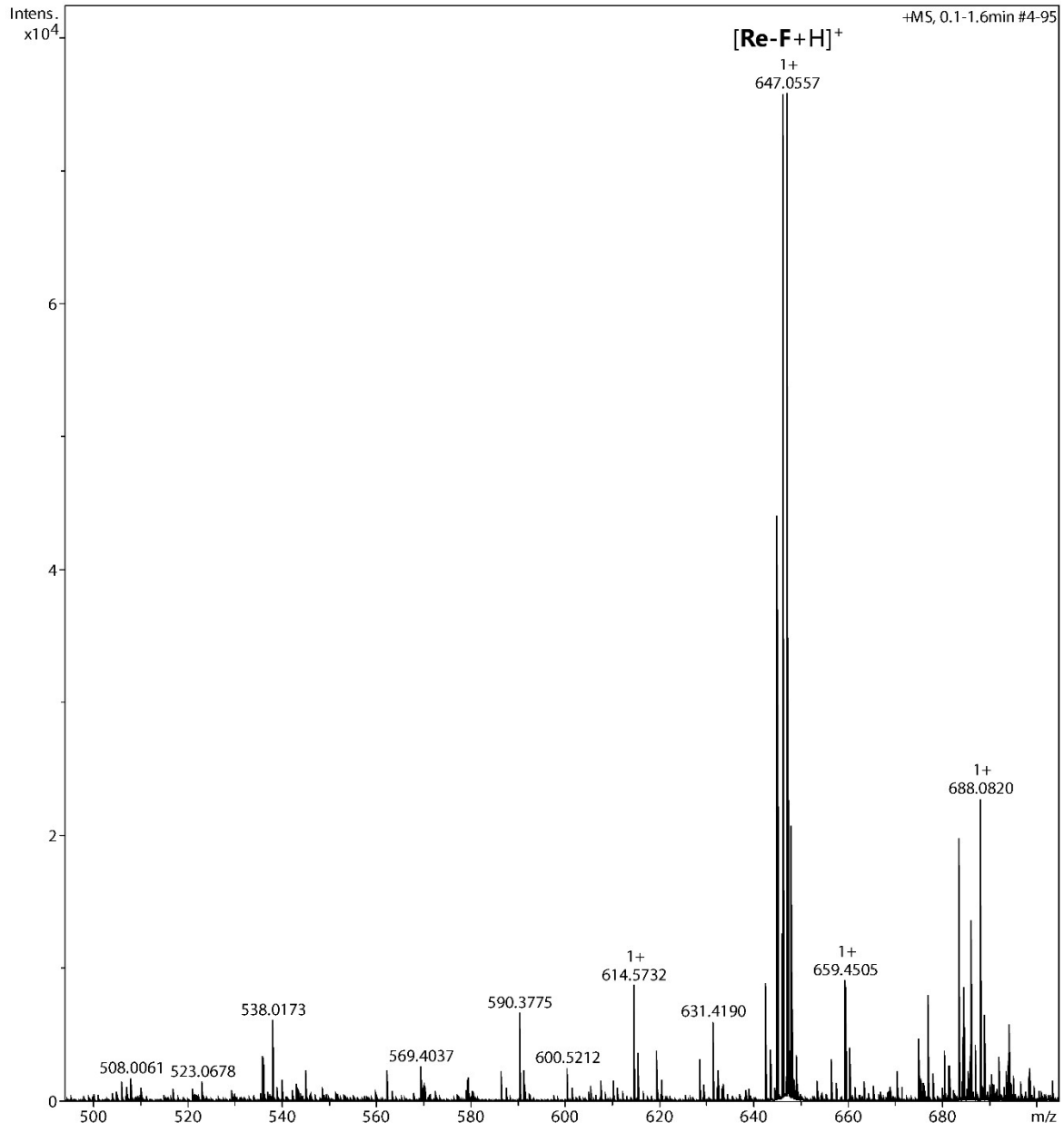

Fig. S2 Experimental ESI mass spectrum of [**Re-F** + H]$^+$ in positive ion mode.

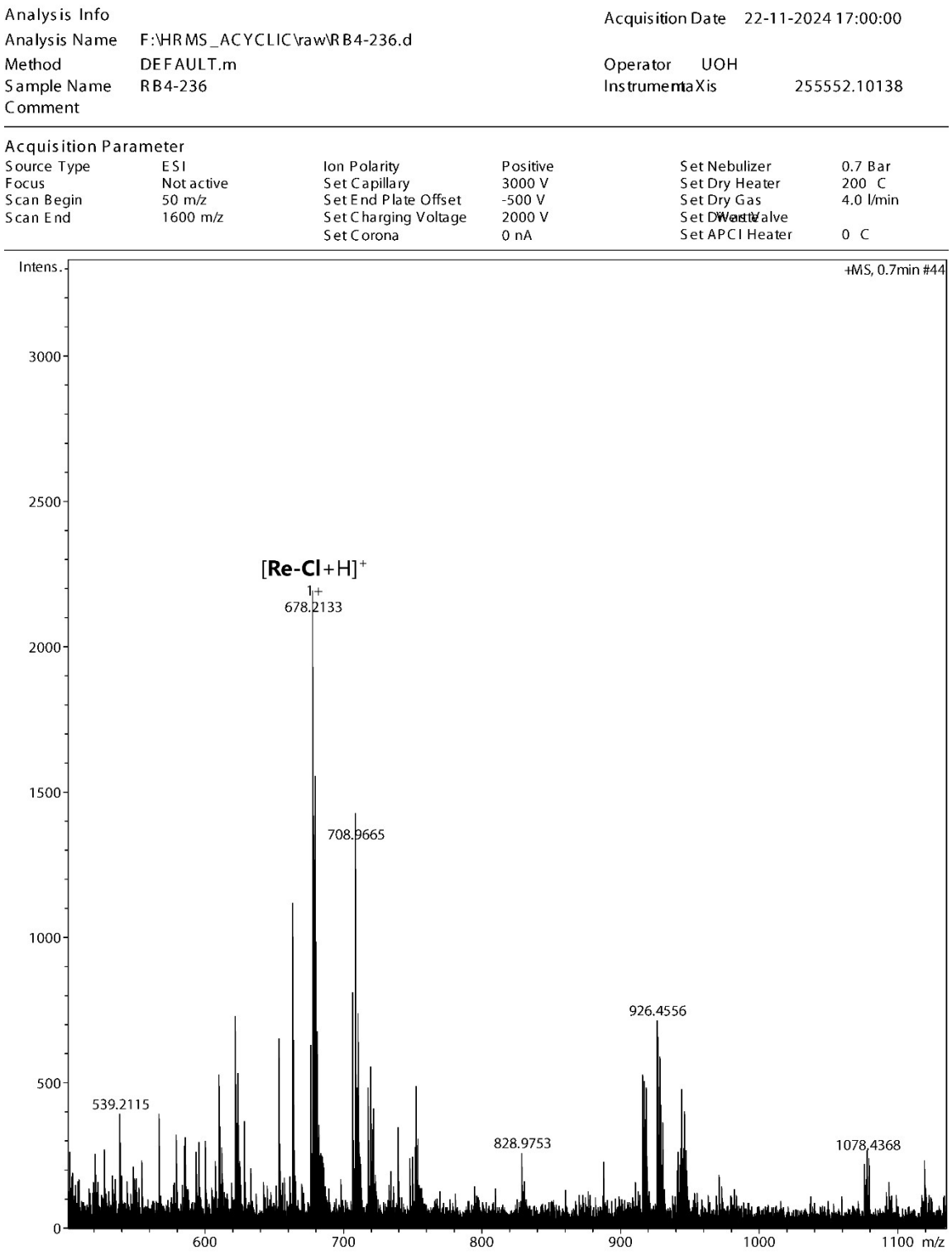

Fig. S3 Experimental ESI mass spectrum of [**Re-Cl** + H]$^+$ in positive ion mode.

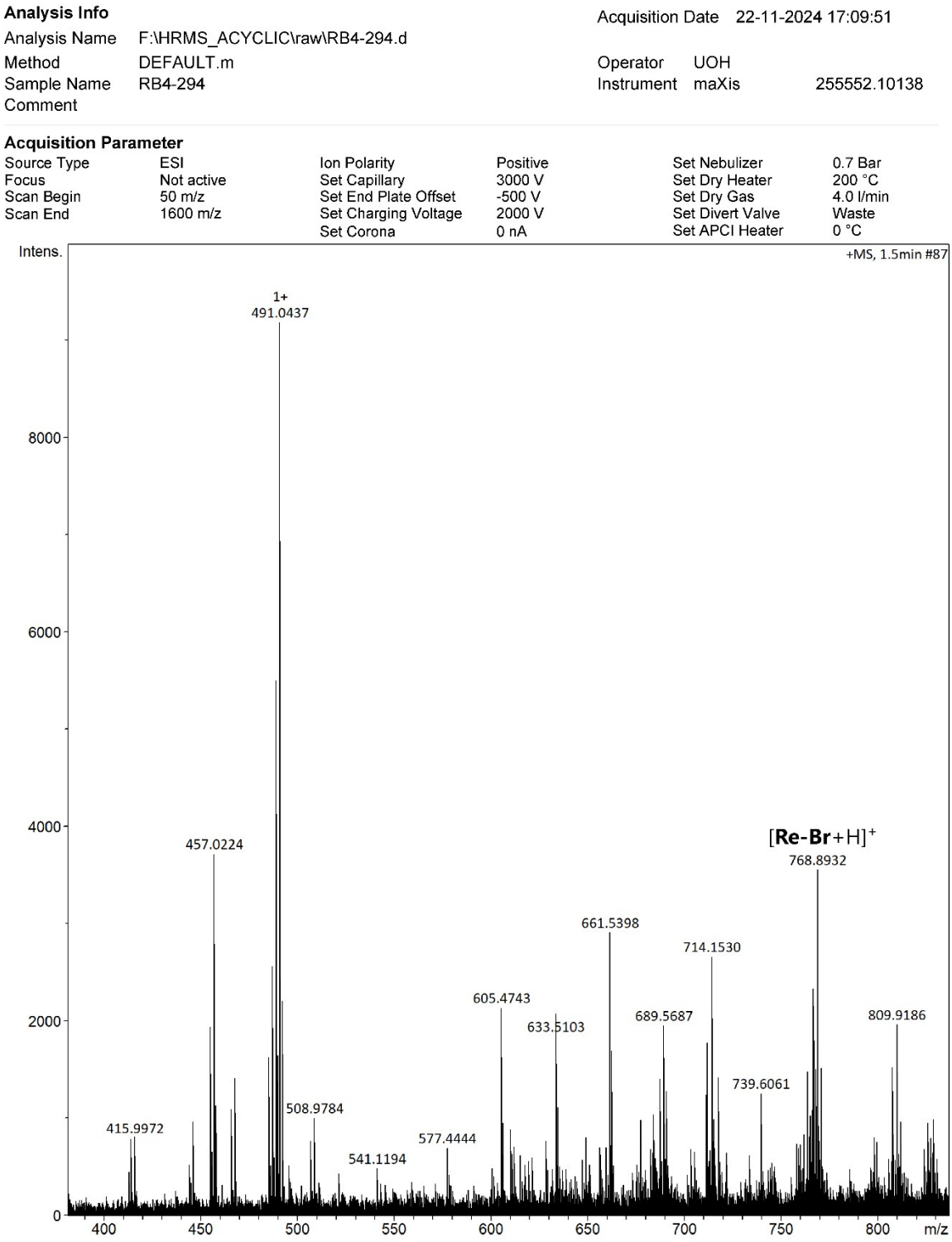

Fig. S4 Experimental ESI mass spectrum of [**Re-Br** + H]$^+$ in positive ion mode.

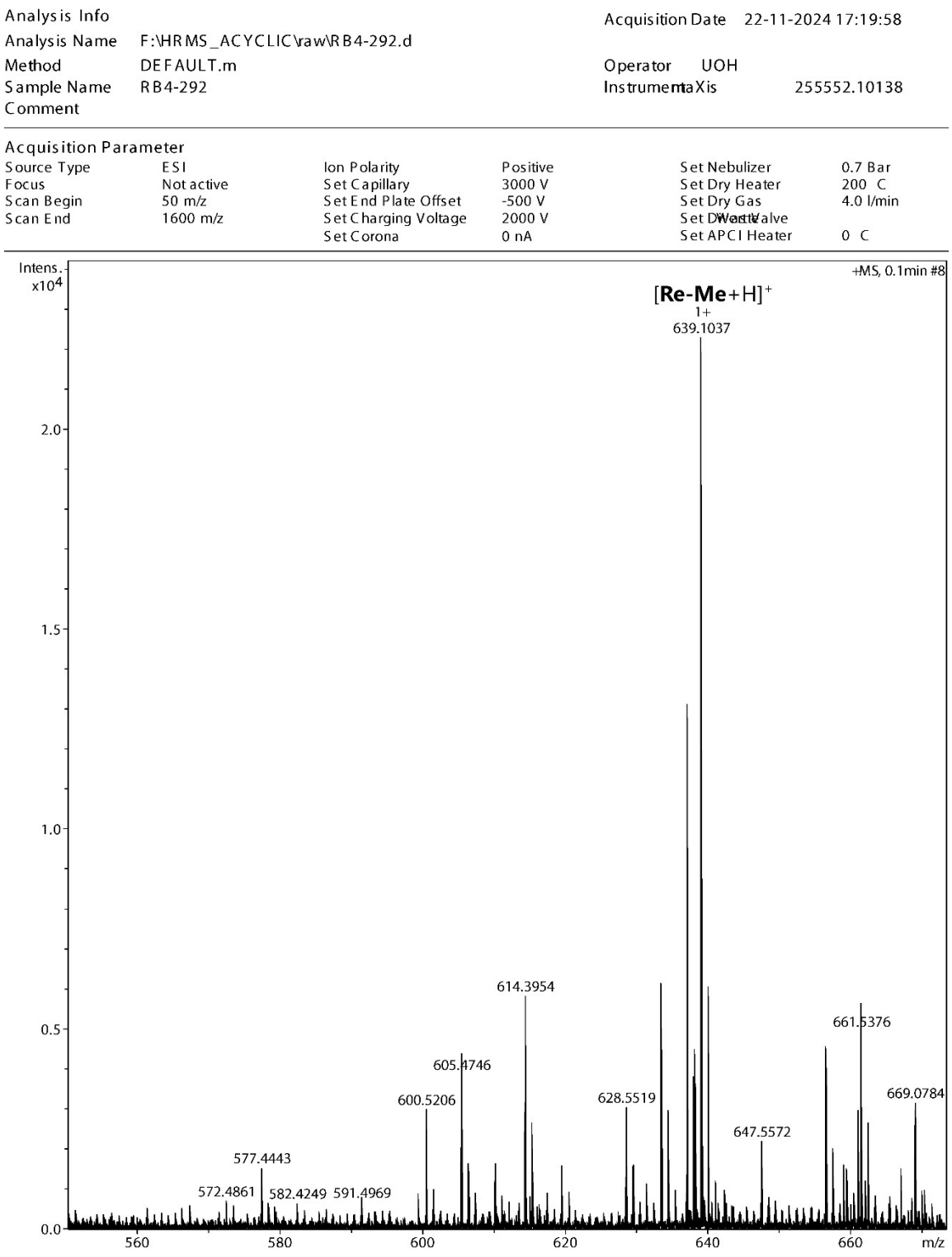

Fig. S5 Experimental ESI mass spectrum of [**Re-Me** + H]$^+$ in positive ion mode.

Analysis Info

Analysis Name	F:\HRMS_ACYCLIC\raw\RB4-240.d	Acquisition Date	22-11-2024 17:14:39
Method	DEFAULT.m	Operator	UOH
Sample Name	RB4-240	Instrument	maXis 255552.10138
Comment			

Acquisition Parameter

Source Type	ESI	Ion Polarity	Positive	Set Nebulizer	0.7 Bar
Focus	Not active	Set Capillary	3000 V	Set Dry Heater	200 °C
Scan Begin	50 m/z	Set End Plate Offset	-500 V	Set Dry Gas	4.0 l/min
Scan End	1600 m/z	Set Charging Voltage	2000 V	Set Divert Valve	Waste
		Set Corona	0 nA	Set APCI Heater	0 °C

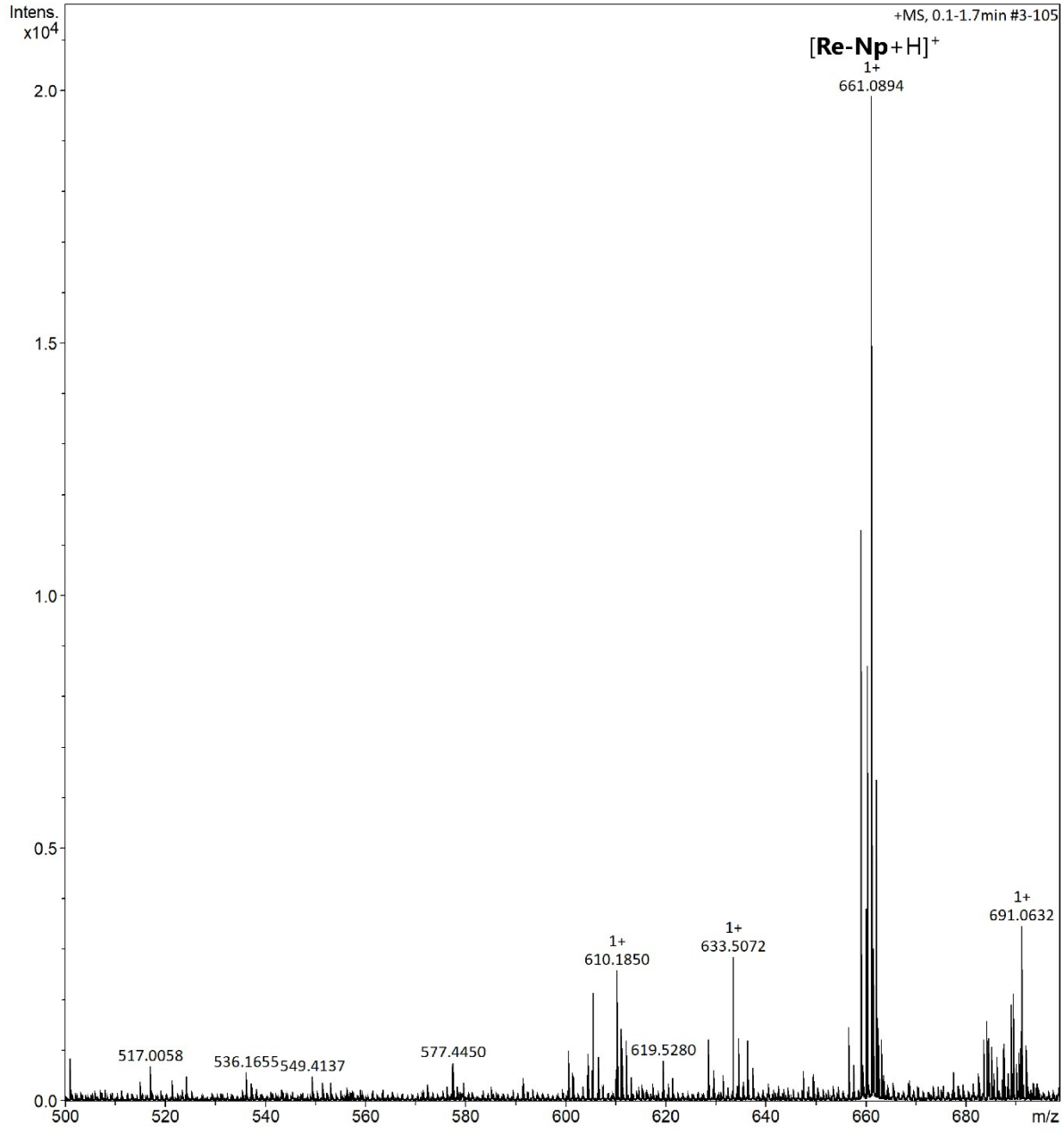

Fig. S6 Experimental ESI mass spectrum of [**Re-Np** + H]$^+$ in positive ion mode.

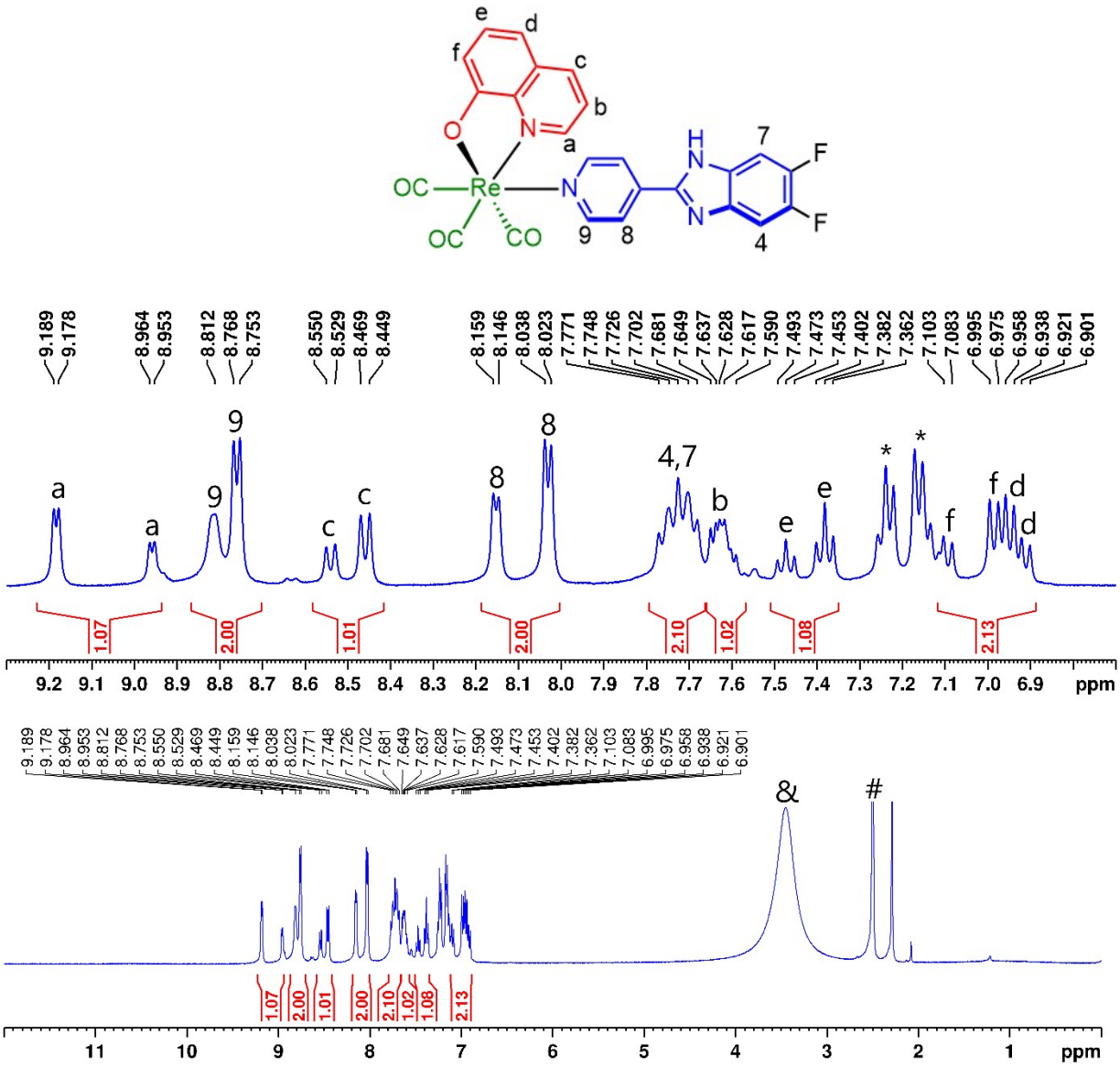

Fig. S7 ^{1}H NMR spectrum of **Re-F** in DMSO-d_6 (* = toluene, # = DMSO-d_6, & = residual H_2O).

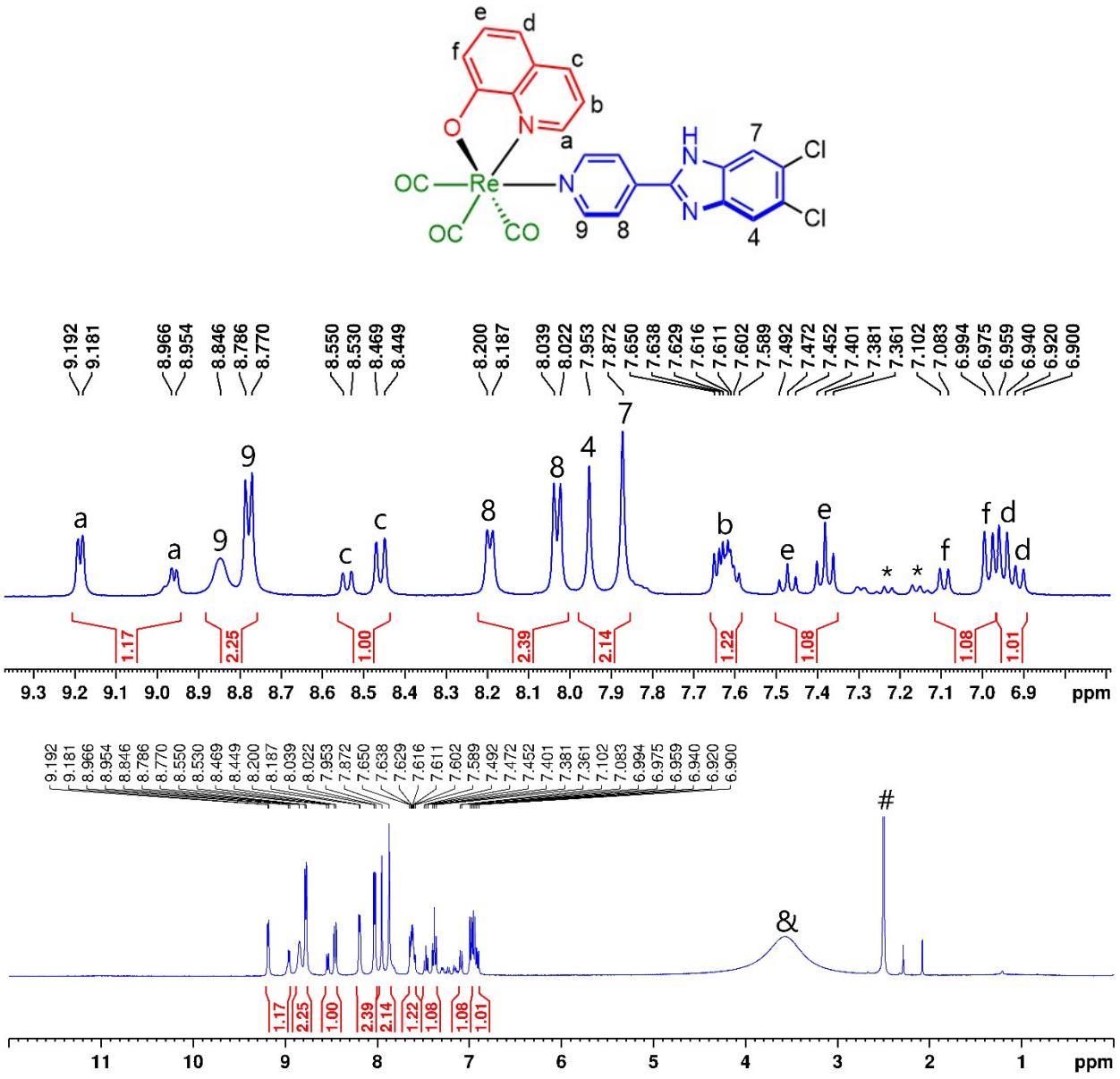

Fig. S8 ^{1}H NMR spectrum of **Re-Cl** in DMSO-d_6 (* = toluene, # = DMSO-d_6, & = residual H_2O).

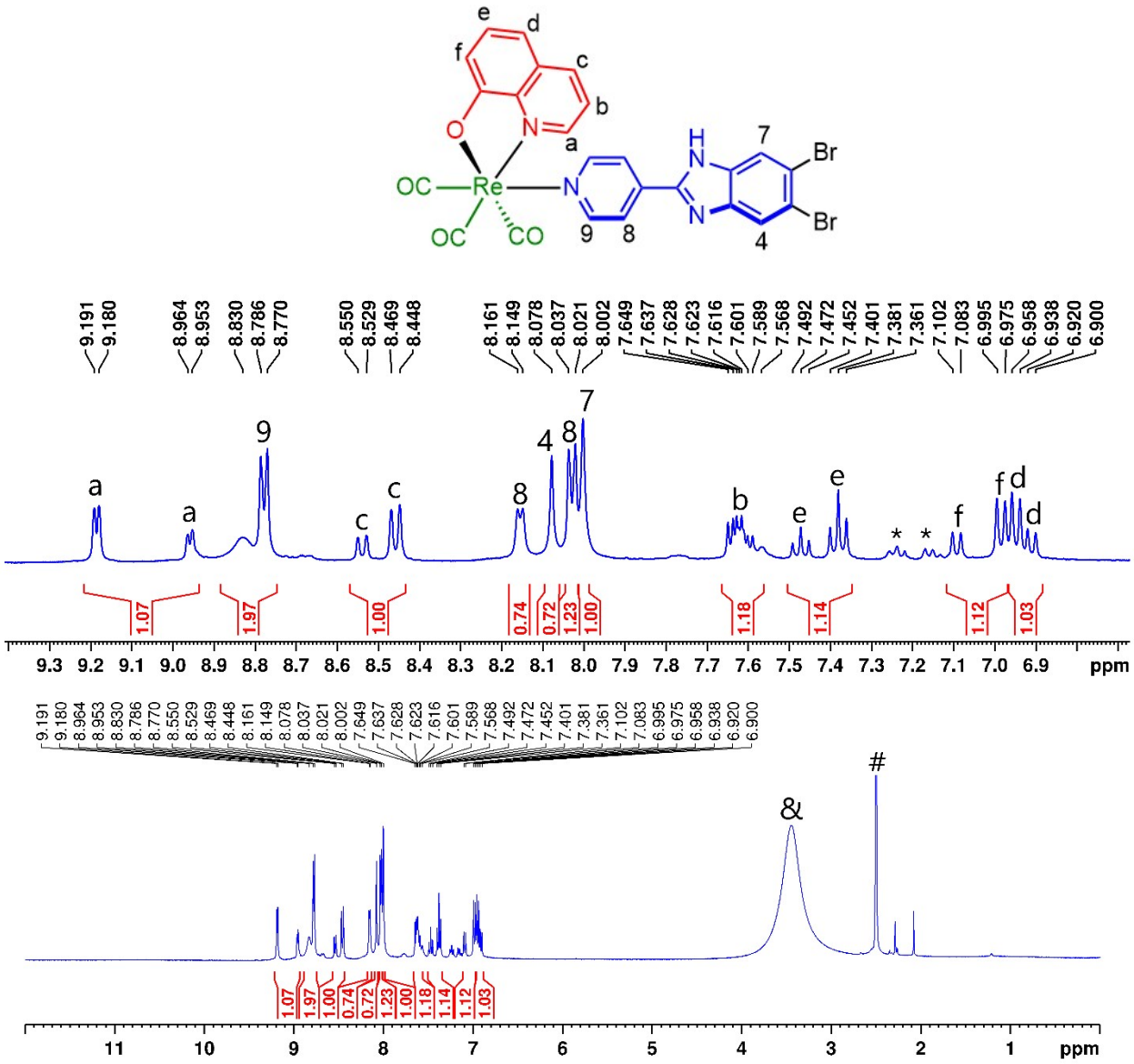

Fig. S9 ^{1}H NMR spectrum of **Re-Br** in DMSO-d_6 (* = toluene, # = DMSO-d_6, & = residual H_2O).

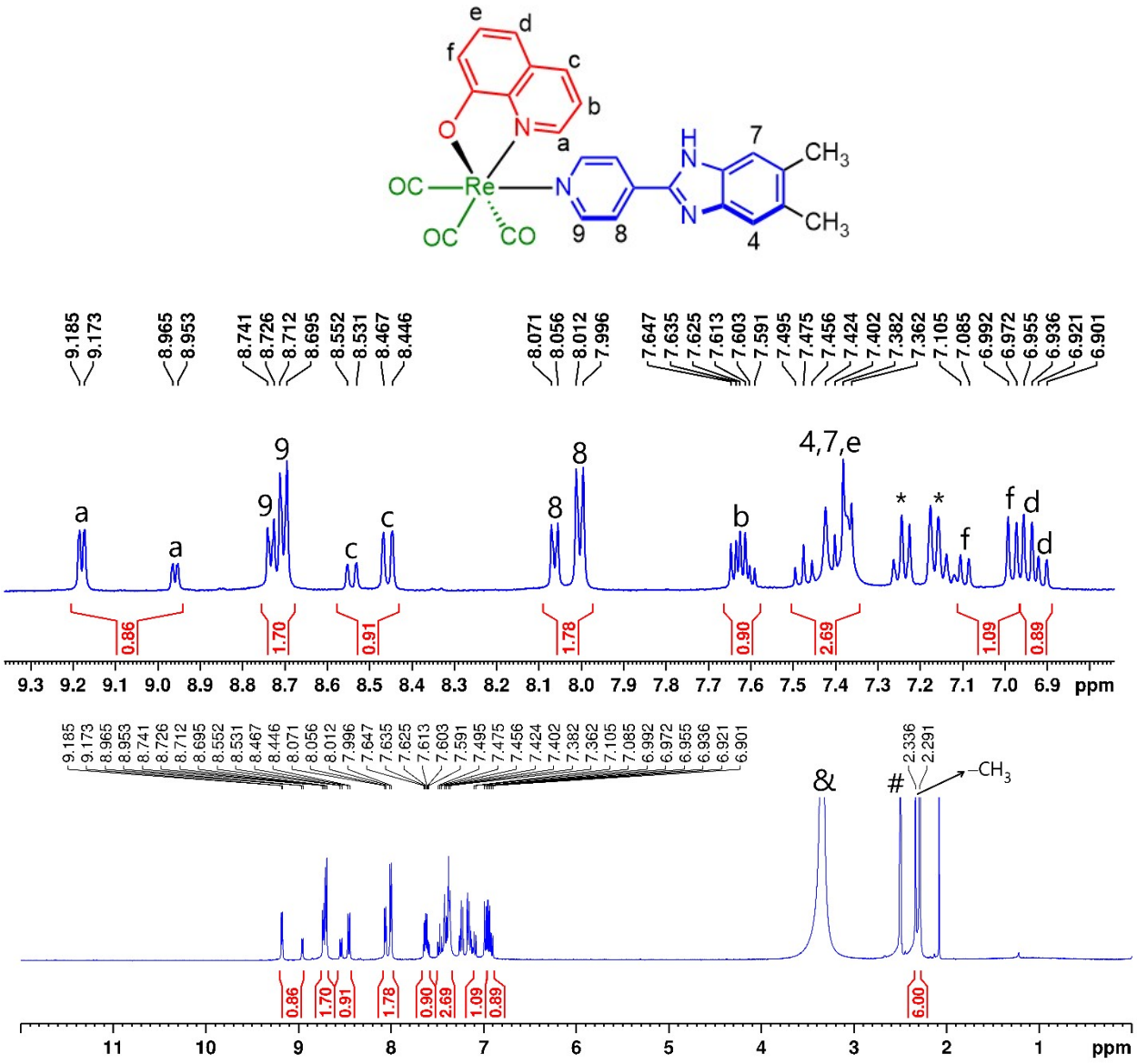

Fig. S10 ^{1}H NMR spectrum of **Re-Me** in DMSO-d_6 (* = toluene, # = DMSO-d_6, & = residual H_2O).

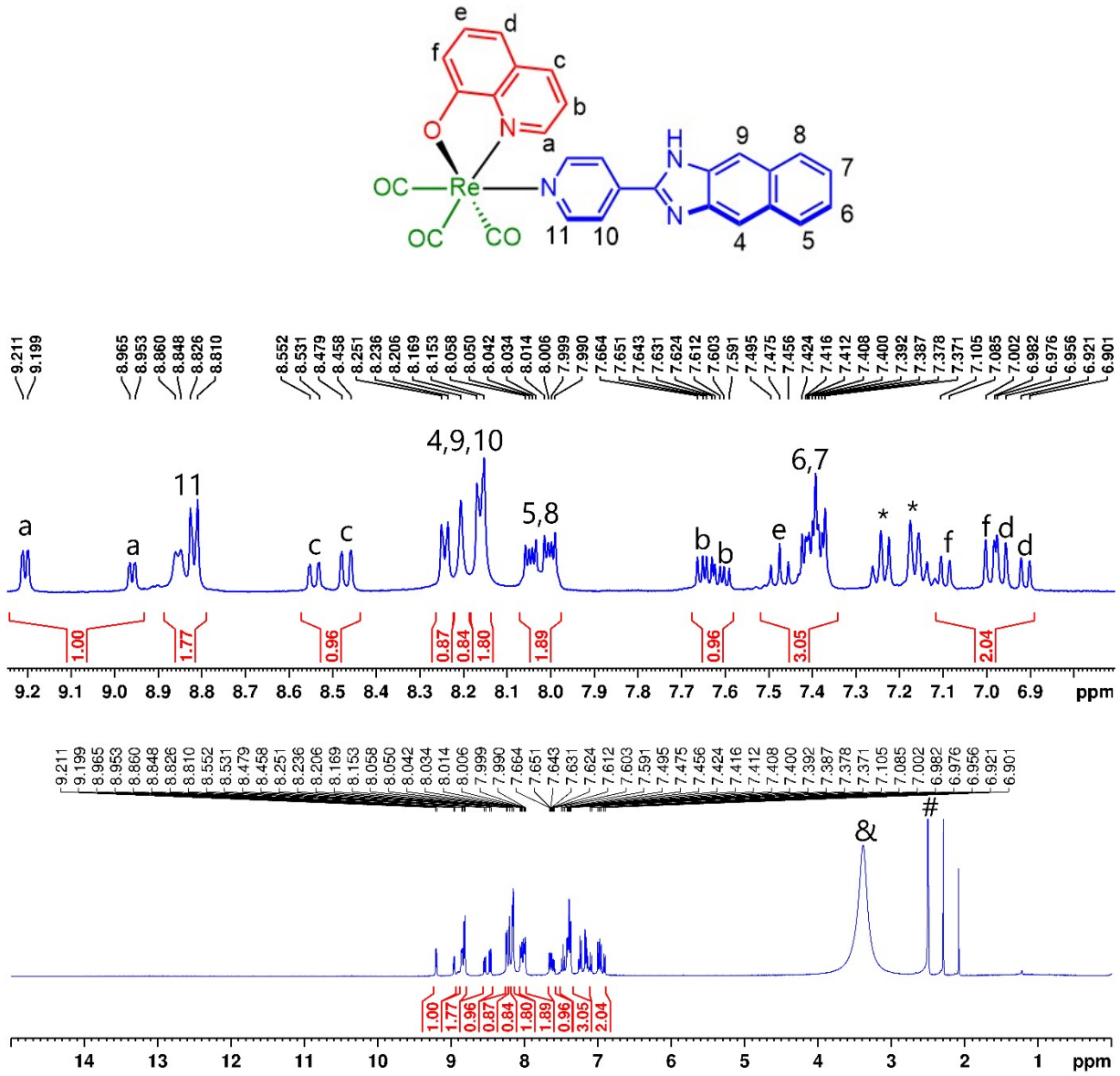

Fig. S11 ^{1}H NMR spectrum of **Re-Np** in DMSO-d_6 (* = toluene, # = DMSO-d_6, & = residual H_2O).

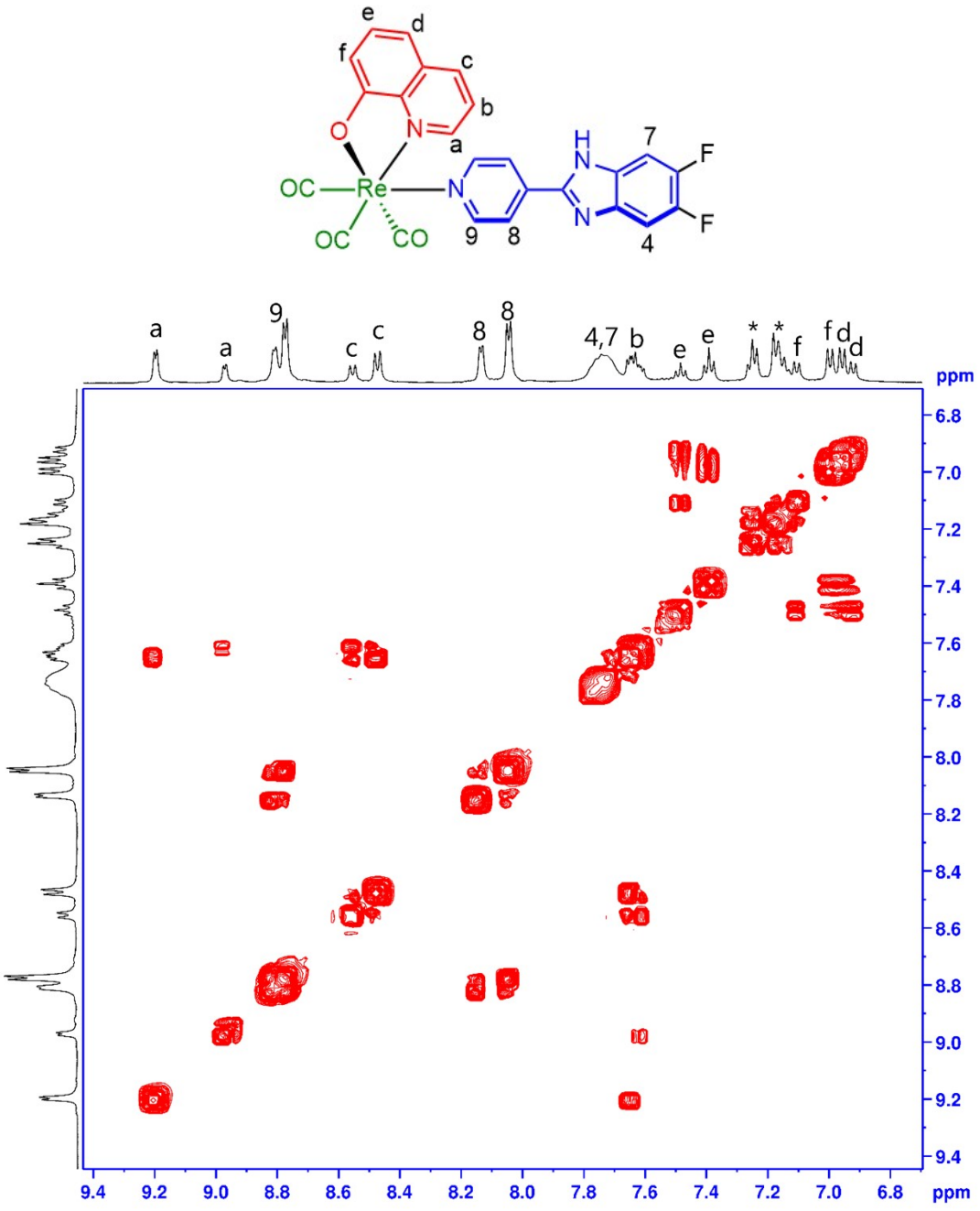

Fig. S12 ^{1}H-^{1}H COSY NMR spectrum of **Re-F** in DMSO-d_6 (∗ = toluene).

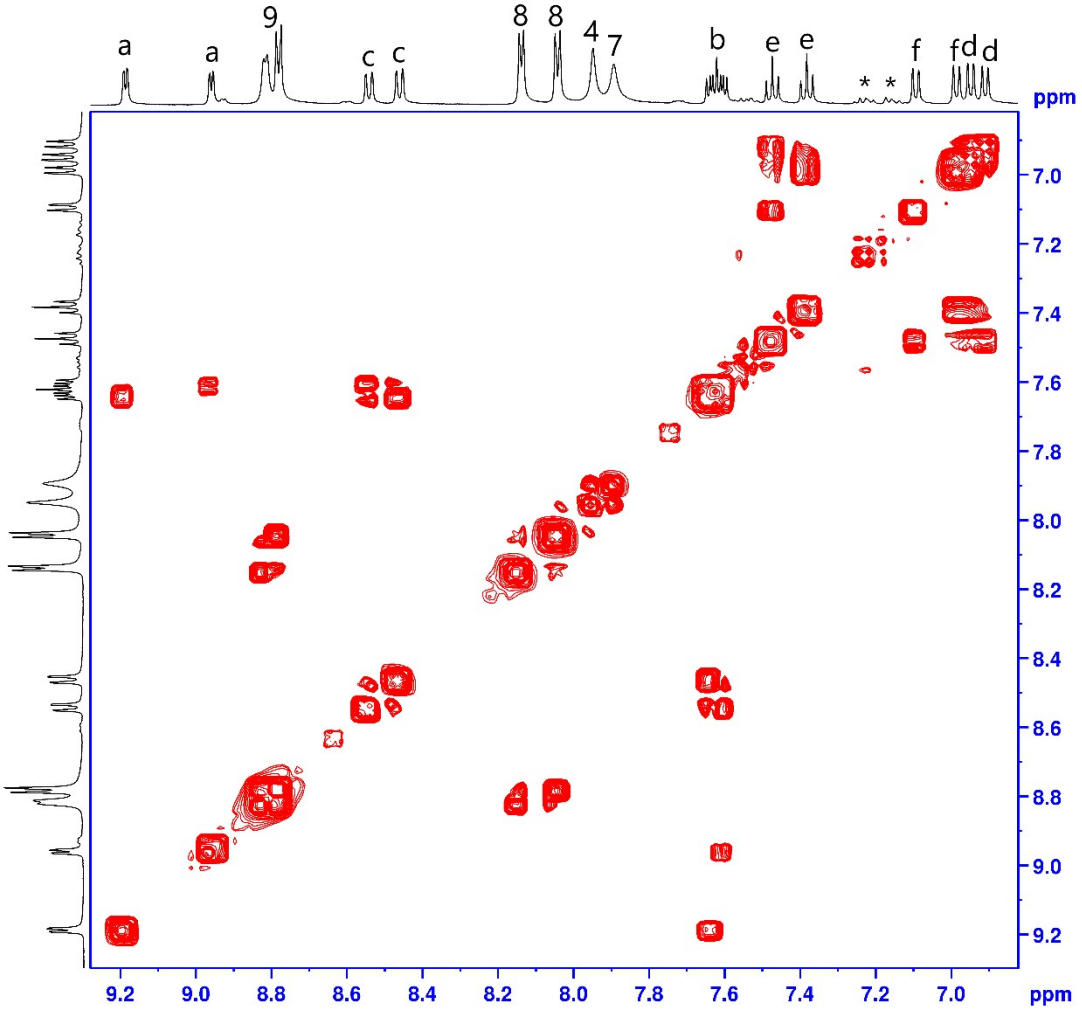

Fig. S13 ^{1}H-^{1}H COSY NMR spectrum of **Re-Cl** in DMSO-d_6 (∗ = toluene).

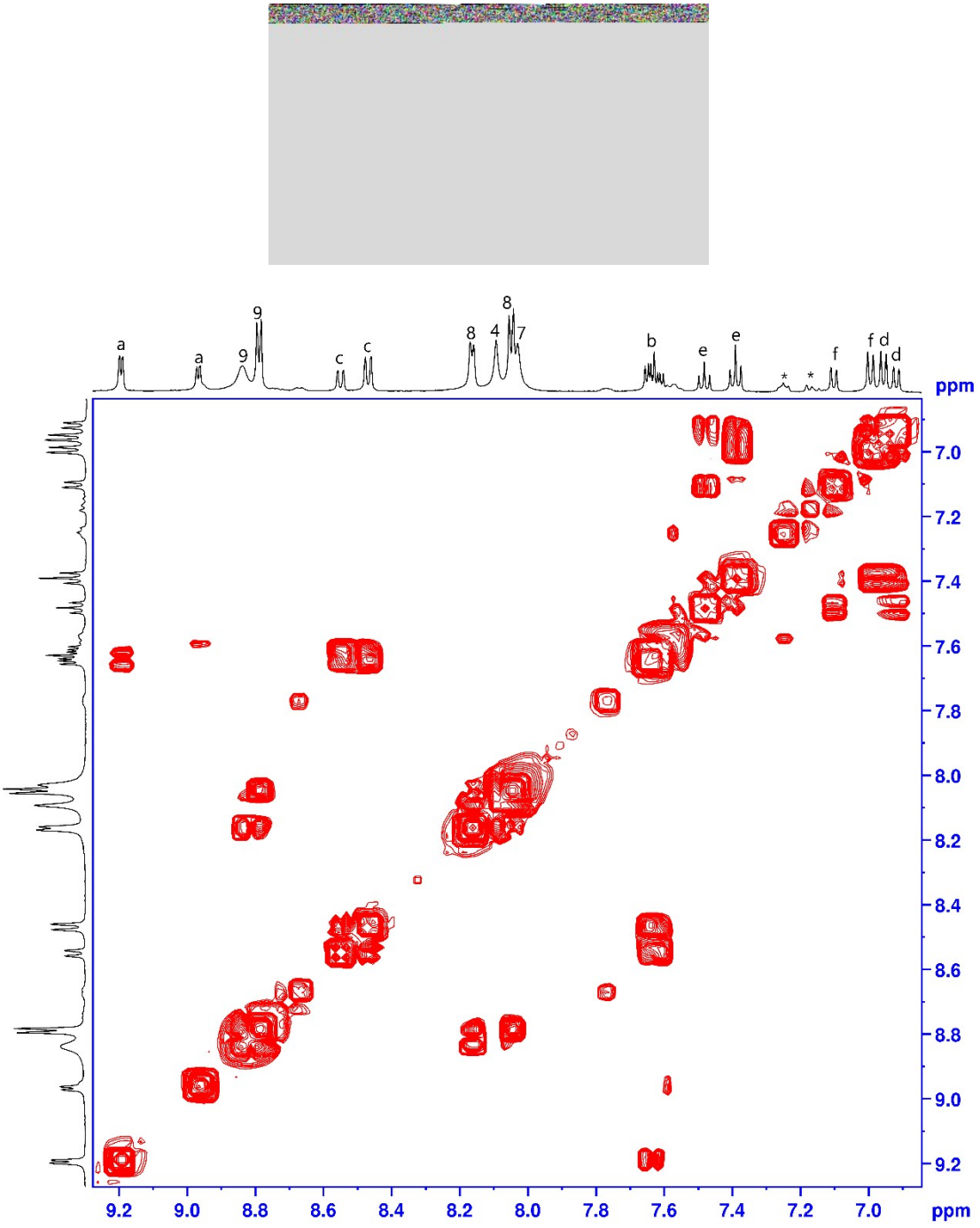

Fig. S14 ^{1}H-^{1}H COSY NMR spectrum of **Re-Br** in DMSO-d_6 (∗ = toluene).

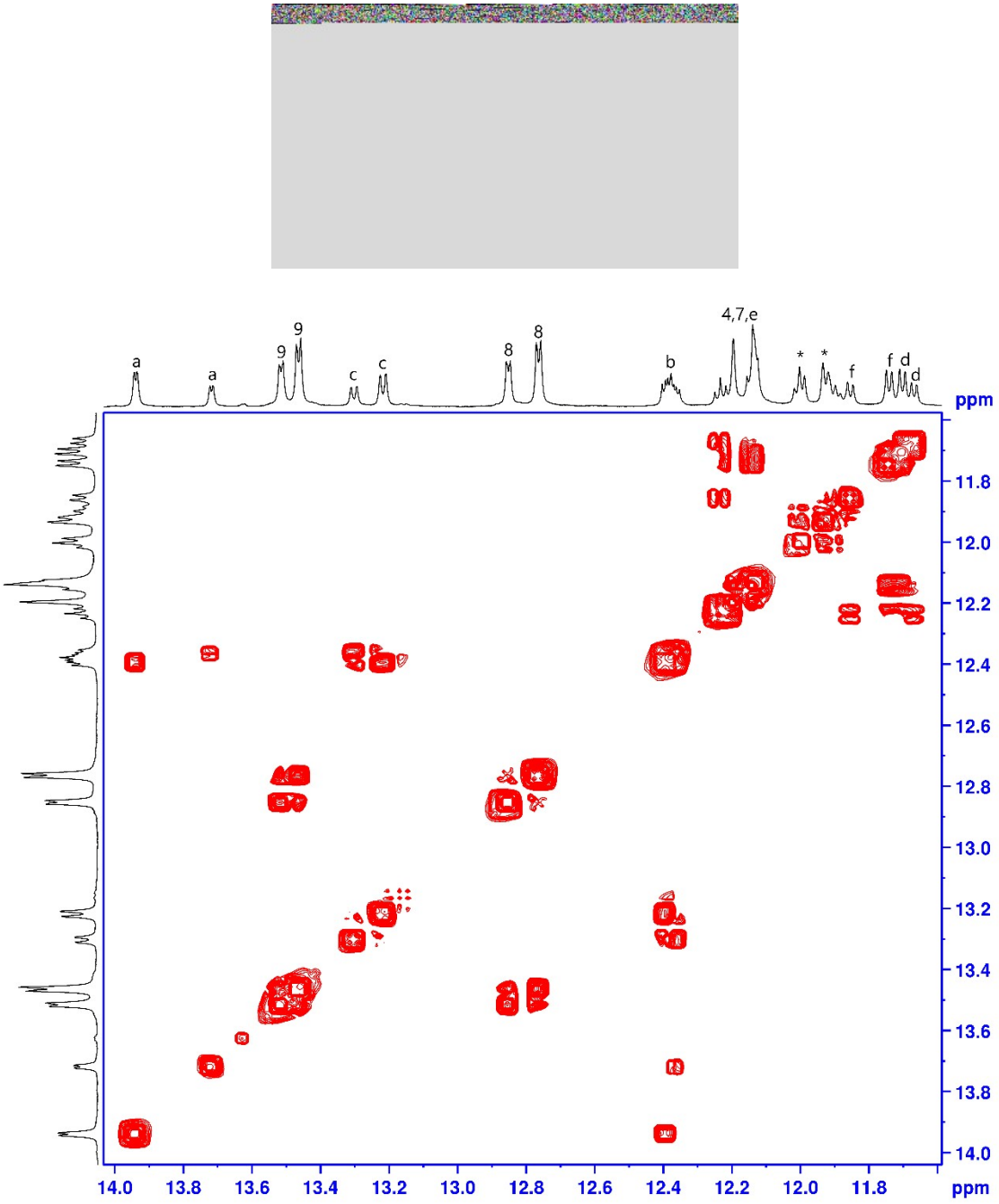

Fig. S15 ^{1}H-^{1}H COSY NMR spectrum of **Re-Me** in DMSO-d_6 (∗ = toluene).

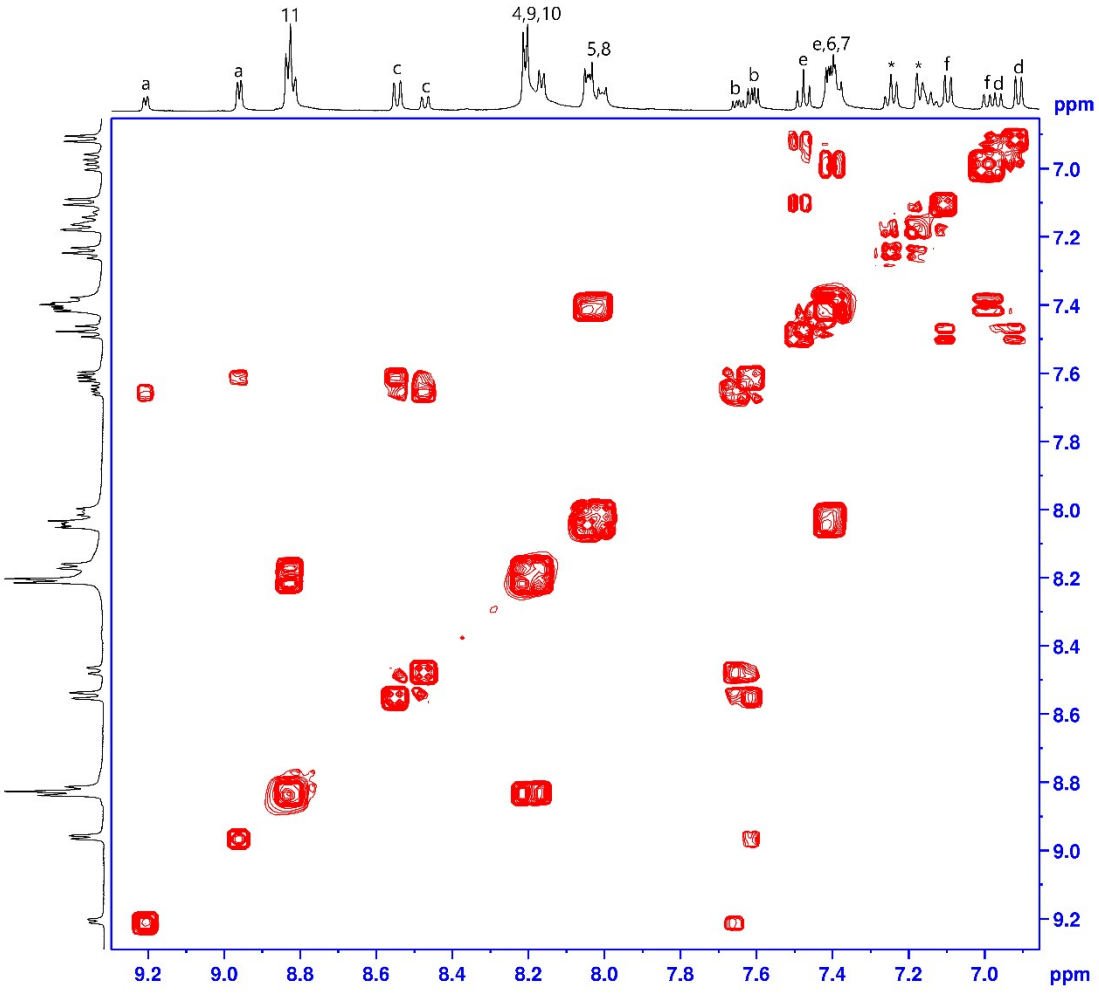

Fig. S16 ^{1}H-^{1}H COSY NMR spectrum of **Re-Np** in DMSO-d_6 (∗ = toluene).

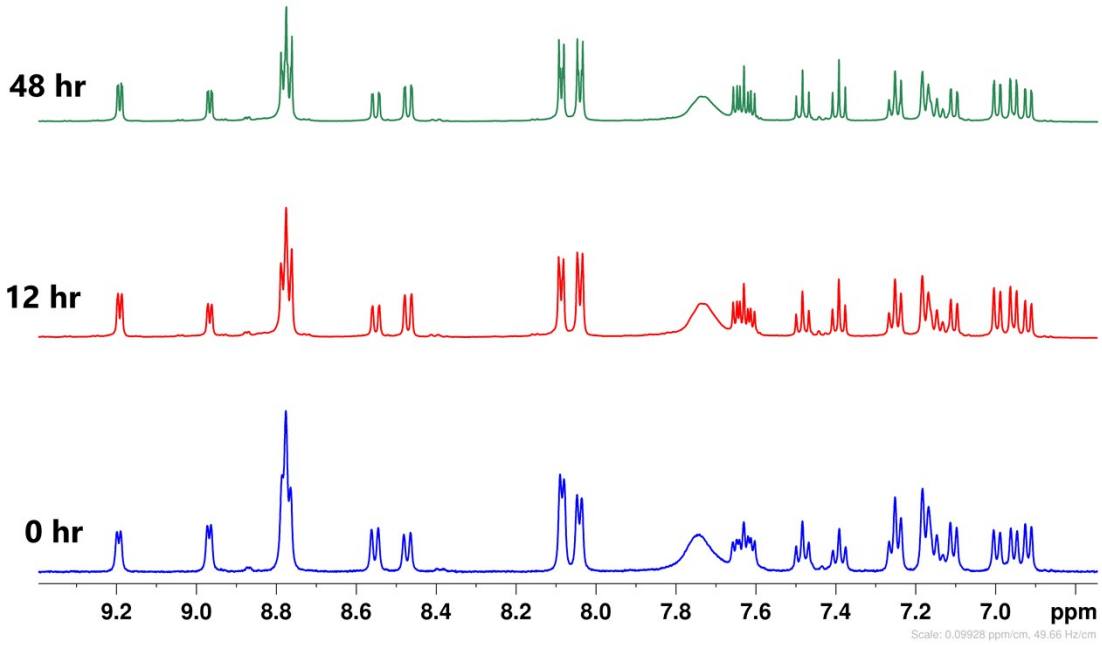

Fig. S17 Partial ^{1}H NMR spectra of complex **Re-F** in DMSO-d_6 showing stability up to 48 hr.

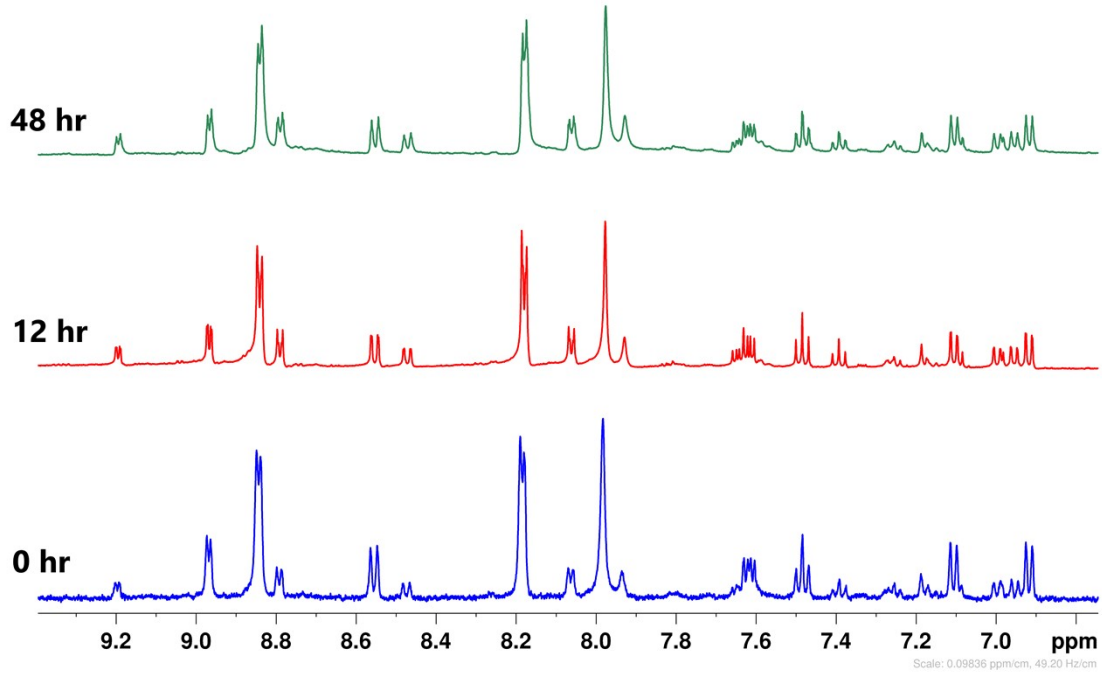

Fig. S18 Partial ^{1}H NMR spectra of complex **Re-Cl** in DMSO-d_6 showing stability up to 48 hr.

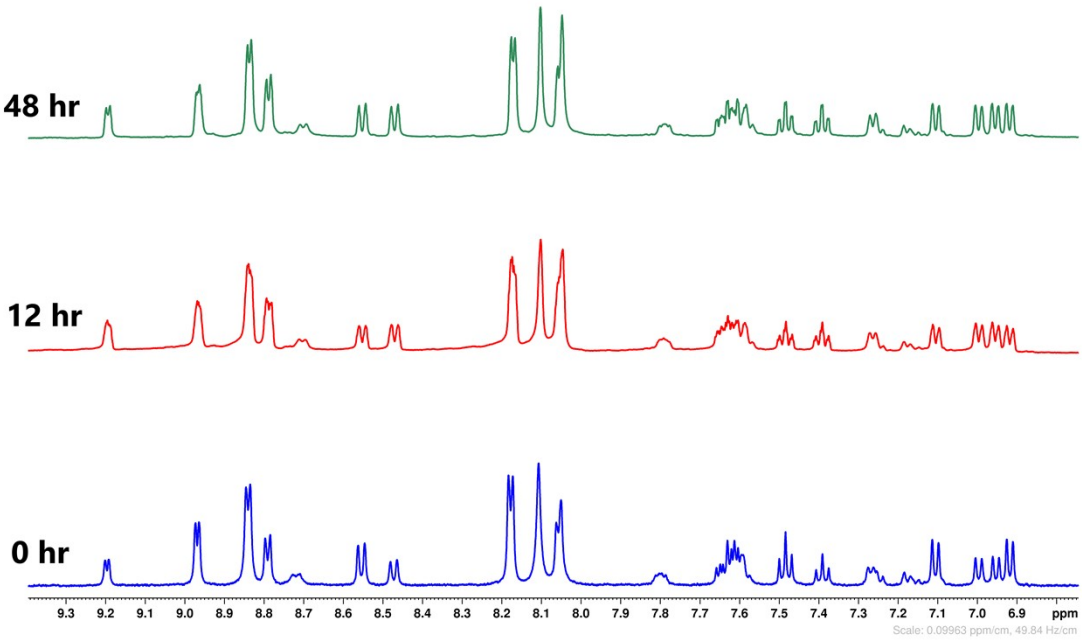

Fig. S19 Partial ^{1}H NMR spectra of complex **Re-Br** in DMSO-d_6 showing stability up to 48 hr.

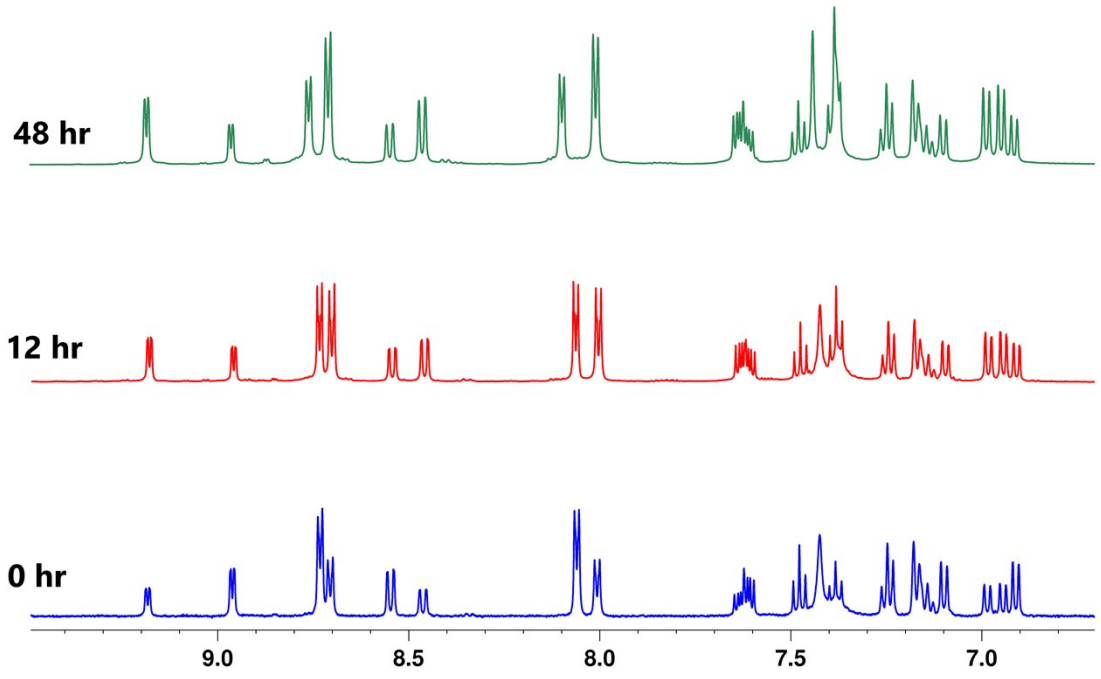

Fig. S20 Partial ^{1}H NMR spectra of complex **Re-Me** in DMSO-d_6 showing stability up to 48 hr.

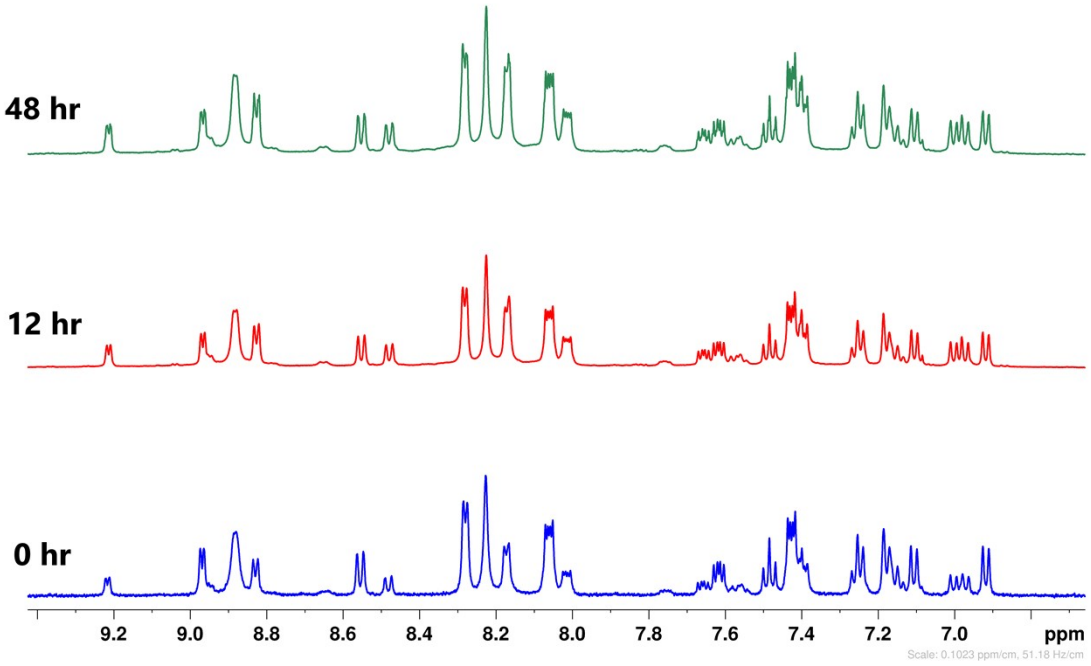

Fig. S21 Partial ^{1}H NMR spectra of complex **Re-Np** in DMSO-d_6 showing stability up to 48 hr.

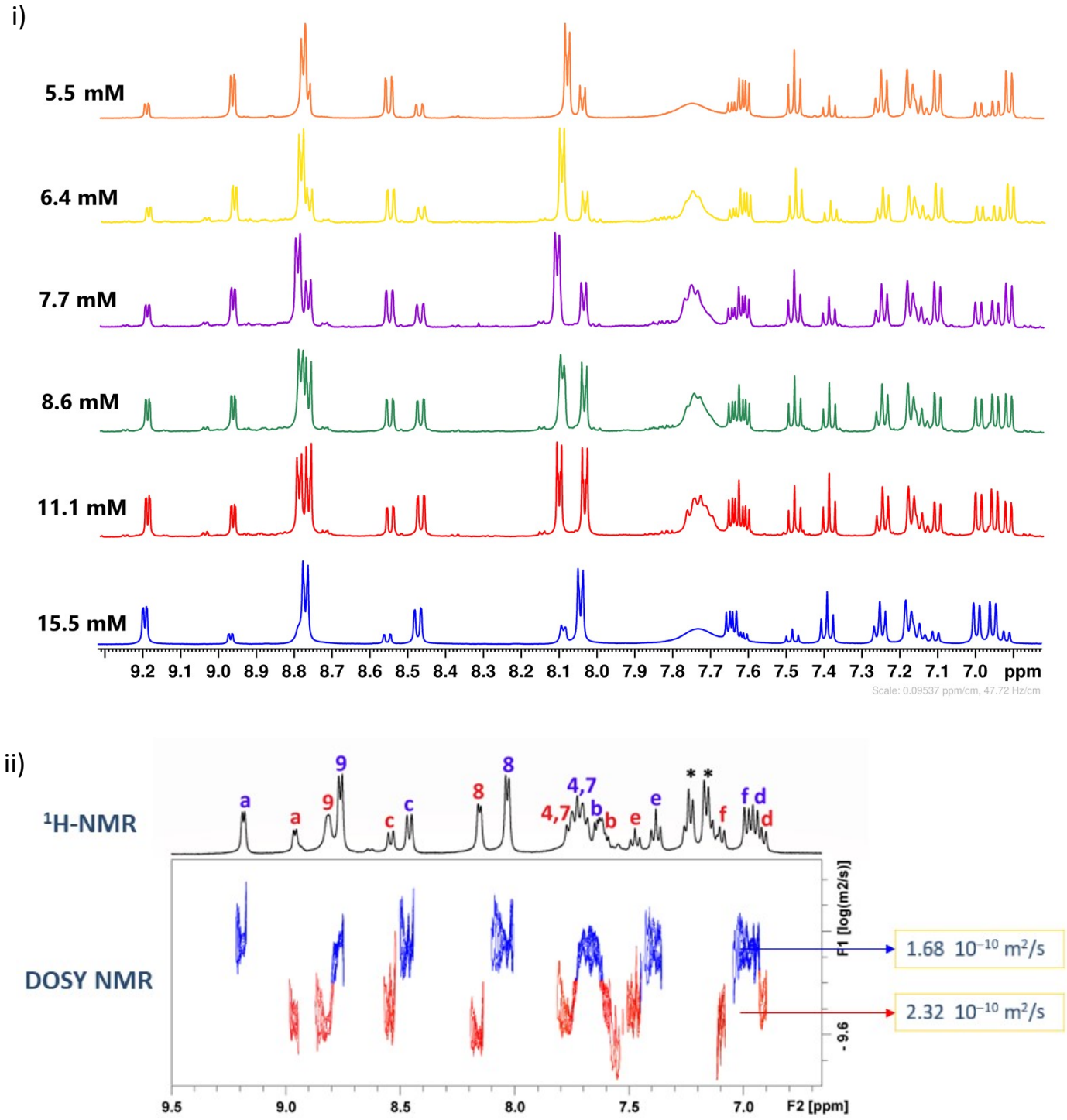

Fig. S22 i) Concentration-dependent partial ^{1}H NMR spectra of complex **Re-F** in DMSO-d_6, ii) ^{1}H NMR and DOSY NMR spectra of complex **Re-F** in DMSO-d_6.

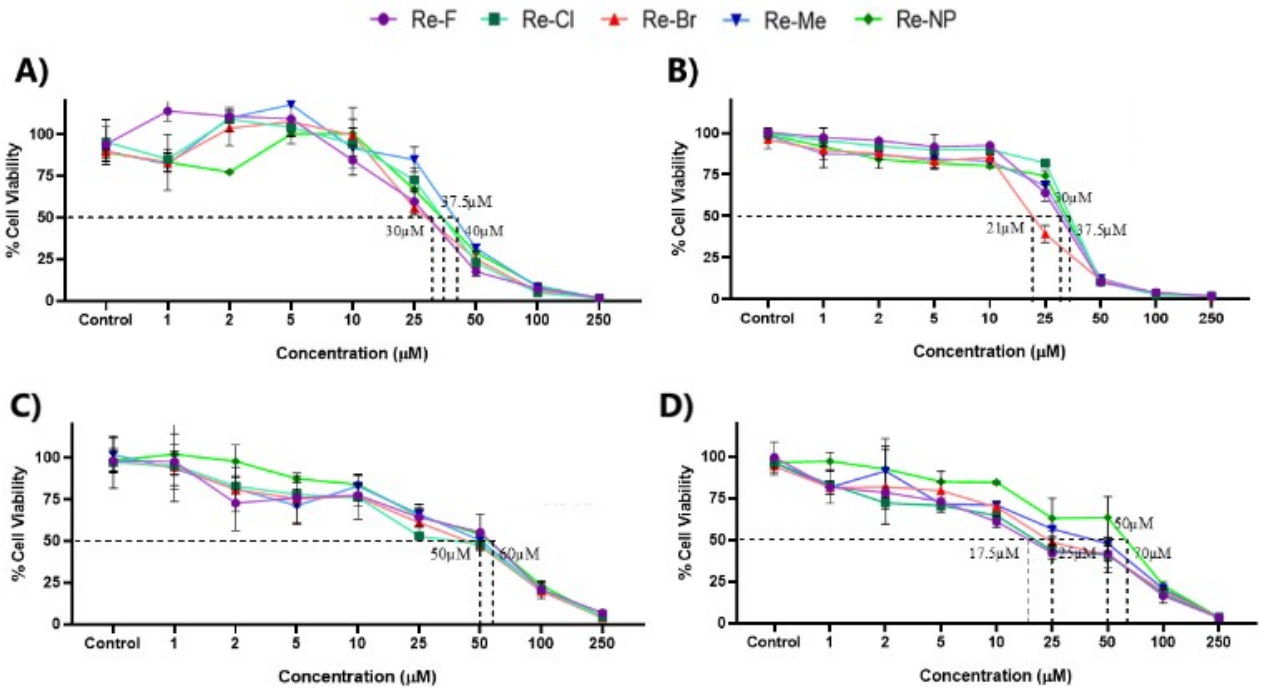

Fig. S23 IC_{50} values of the complexes determined using MTT assay towards noncancer cell lines (A: L929, B: NIH 3T3, C: H9C2, and D: C2C12).

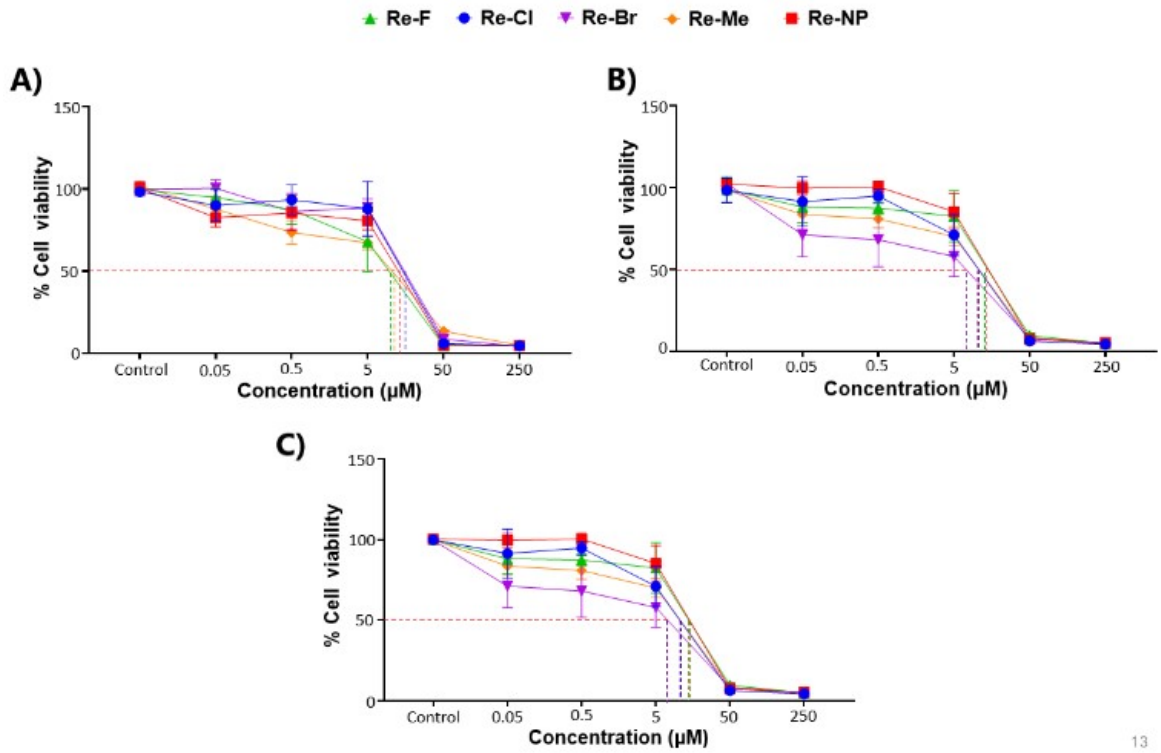

Fig. S24 IC_{50} values of the complexes determined using MTT assay towards cancer cell lines (A: 4T1, B: A549, and C: HeLa).

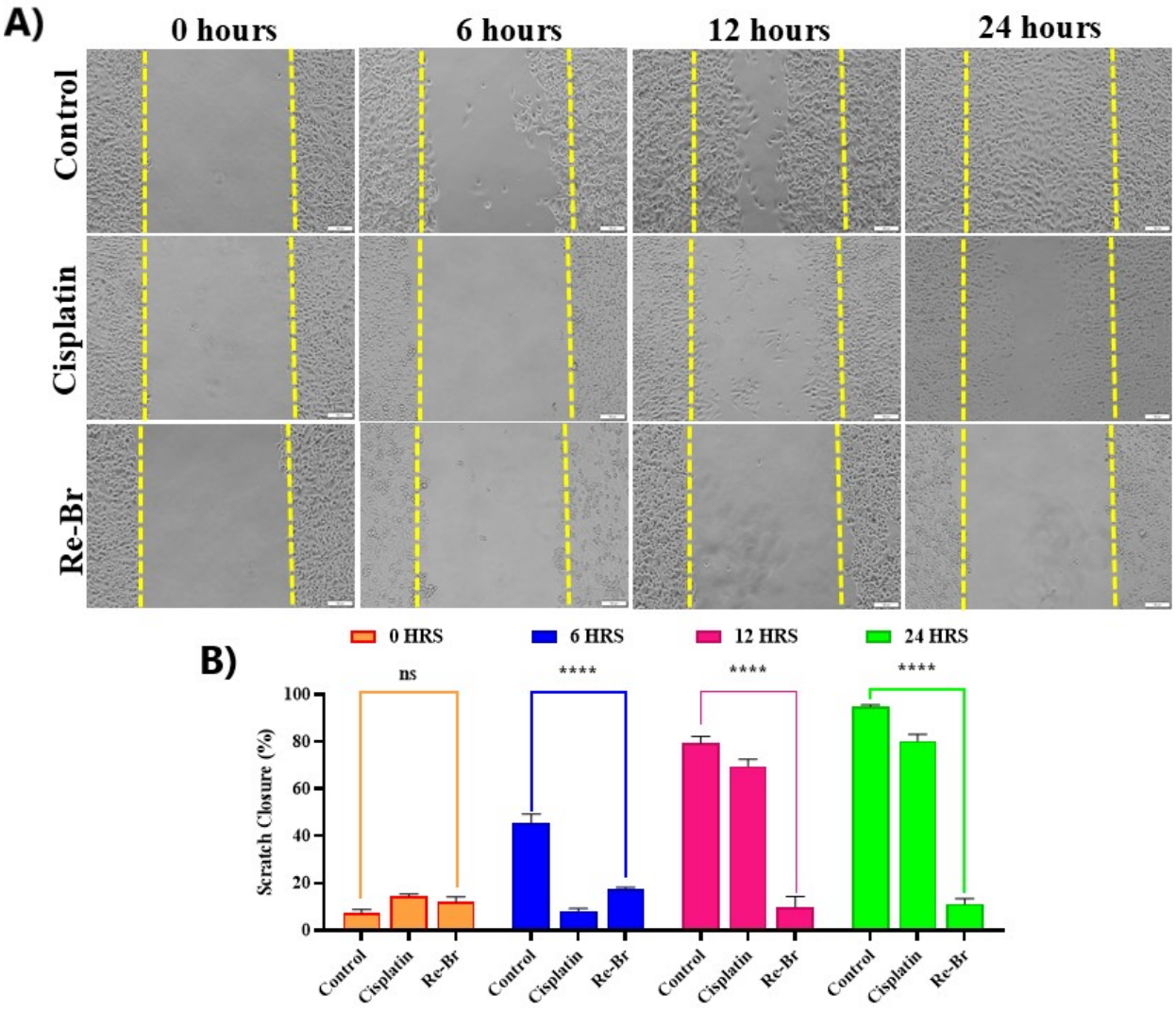

Fig. S25 (A) Evaluation of antimetastatic effects of **Re-Br** on HeLa cells using scratch assay, untreated cells (negative control), and Cisplatin (positive control) (Scale bar: 100 μm). (B) Percentage of scratch closure at 0, 6, 12 and 24 hr of treatment.

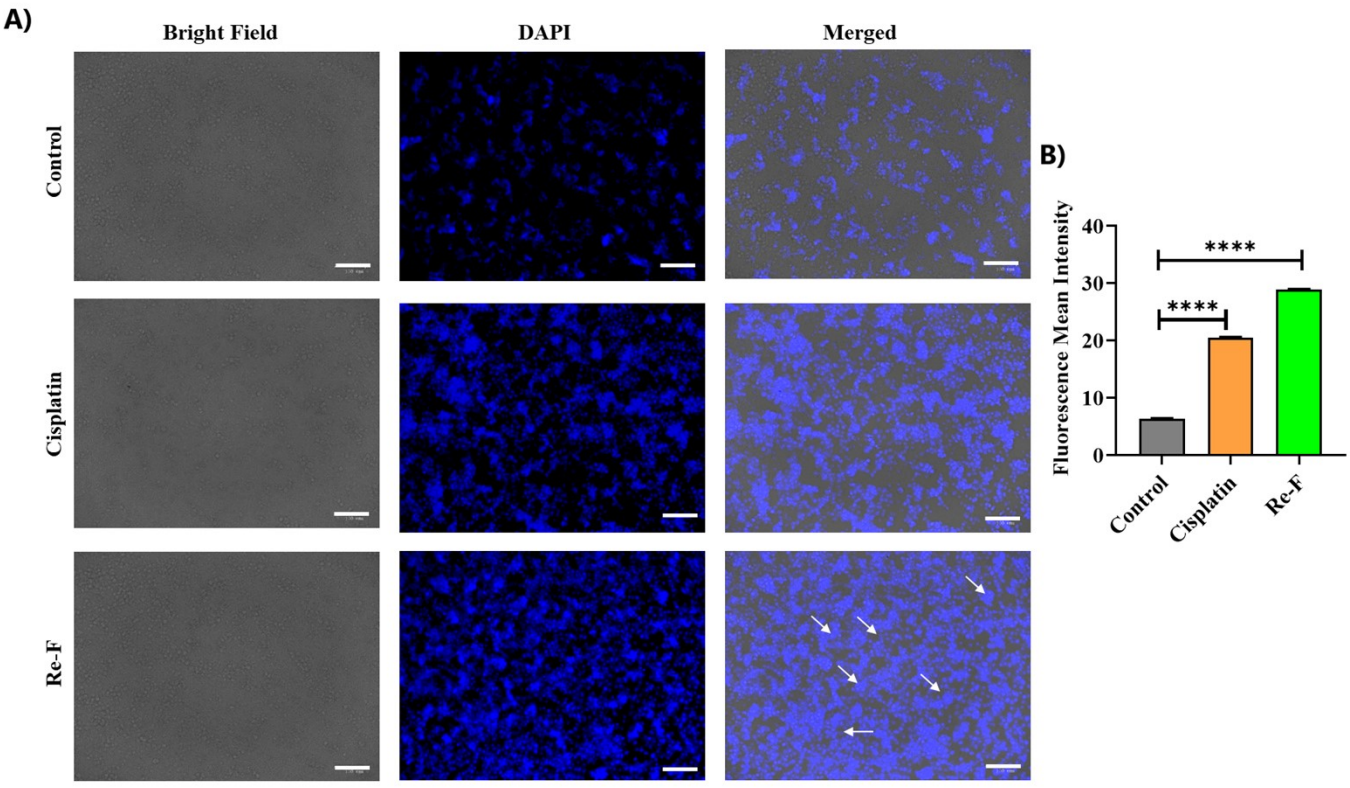

Fig. S26 (A) Detection of DNA damage after being treated with **Re-F** and cisplatin. Control (Untreated 4T1 cells) was used as a negative control and cells treated with cisplatin were used as a positive control (Scale bar: 20 μm). (B) Quantification data of fluorescence intensity.

Table S1 Crystal data and structure refinement for the complexes

Crystal data	**Re-F·0.5(C_7H_8)**	**Re-Cl**	**Re-Br**
Empirical	$2(C_{24}H_{13}F_2N_4O_4Re)\cdot C_7H_8$	$C_{24}H_{13}Cl_2N_4O_4Re$	$C_{24}H_{13}Br_2N_4O_4Re$
Formula Mass	1383.30	678.48	767.40
Crystal system	Triclinic	Monoclinic	Monoclinic
Space group	$P\bar{1}$	*P21/c*	*P21/c*
a (Å)	8.2524(12)	13.5446(8)	13.6752(16)
b (Å)	13.0329(17)	12.4925(7)	12.6834(15)
c (Å)	13.224(2)	13.8159(8)	13.9947(15)
α (°)	63.168(5)	90	90
β (°)	89.537(6)	102.226(2)	103.896(4)
γ (°)	81.939(6)	90	90
V (Å^3)	1254.1(3)	2284.7(2)	2356.3(5)
d (g/cm^3)	1.832	1.973	2.163
Z	1	4	4
T (K)	296(2)	194(2)	296(2)
R factor (*I* >	0.0187	0.0360	0.0297
wR_2 ($I > 2\sigma(I)$)	0.0492	0.0923	0.0675
R factor (all data)	0.0192	0.0402	0.0357
wR_2 (all data)	0.0494	0.0949	0.0700
GooF	1.139	1.037	1.076
CCDC No	**2451110**	**2451108**	**2451107**

Table S2 Crystal data and structure refinement for the complexes

Crystal data	**Re-Me·0.5(C_7H_8)**	**Re-Np·0.5(C_7H_7)**
Empirical Formula	$2(C_{26}H_{19}N_4O_4Re)\cdot C_7H_8$	$2(C_{28}H_{17}N_4O_4Re)\cdot C_7H_7$
Formula Mass	1367.46	1410.44
Crystal system	Triclinic	Triclinic
Space group	$P\bar{1}$	$P\bar{1}$
a (Å)	9.561(3)	9.4326(8)
b (Å)	9.643(2)	9.7541(7)
c (Å)	14.547(4)	14.6129(12)
α (°)	87.588(9)	86.912(3)
β (°)	89.061(10)	88.962(3)
γ (°)	84.671(9)	86.779(3)
V (Å^3)	1334.2(6)	1340.26(19)
d (g/cm^3)	1.702	1.747
Z	1	1
T (K)	294(2)	296(2)
R factor ($I > 2\sigma(I)$)	0.0276	0.0188
wR_2 ($I > 2\sigma(I)$)	0.0764	0.0491
R factor (all data)	0.0283	0.0193
wR_2 (all data)	0.0768	0.0494
GooF	1.213	1.152
CCDC No	**2451111**	**2451109**

Table S3 Selected bond lengths [Å] for the complexes

Complexes					
	Re-F	**Re-Cl**	**Re-Br**	**Re-Me**	**Re-Np**
Re1-C1	1.916(3)	1.897(6)	1.896(6)	1.913(4)	1.898(3)
Re1-C2	1.924(3)	1.902(7)	1.901(6)	1.916(4)	1.921(3)
Re1-C3	1.908(3)	1.901(6)	1.904(6)	1.901(4)	1.900(3)
Re1-N3	2.228(2)	2.209(5)	2.206(4)	2.206(3)	2.214(2)
Re1-N4	2.167(2)	2.171(4)	2.172(4)	2.172(3)	2.171(2)
Re1-O4	2.132(2)	2.128(4)	2.132(3)	2.134(3)	2.1324(19)
N1-H1	0.72(3)	0.80(5)	0.76(6)	0.73(6)	0.73(3)

Supporting Information for Computational theory selection

Various studies use different density functional theory and basis sets.[1-3] To select the most suitable theory, some of the mentioned theories in the articles are used for geometry optimization of the fluorine derivative of the complex (test). The list of theory and basis set used for ground state optimization: 1. B3LYP/LANL2DZ(Re)/6-311++G(d,p), 2. B3PW91/SDDALL(Re)/6-31G(d,p), 3. PBE0/SDDALL(Re)/6-31G(d,p), 4. MO6L/SDDALL(Re)/ 6-31G(d,p), 5. MO6L/LANL2DZ(Re)/6-311++G(d,p), and 6. B3LYP/SDD(Re)/6-311G*. "Theory/basis set 1 (Re)/basis set 2" indicates that particular basis set 1 is used only for Re atoms, and other atoms are computed by the next-mentioned basis set 2. In all the calculations, empirical dispersion is added as GD3BJ. All the calculations have been carried out using Gaussian16 software.[4] The bond distance between the Re atom and the six bonded atoms is measured from the optimized geometry. Then it is compared with fluorine derivative XRD structure. The difference in average bond distance between the XRD result and the optimized result is calculated. The least difference of the optimized geometry result is taken for further computational analysis. Here, it is evident from Table S4 that the B3PW91/SDDALL(Re)/6-31G(d,p) combination is best for the computational study. After optimizing at B3PW91/SDDALL(Re)/6-31G(d,p) level, the obtained geometry was used for the force field parametrization.

Table S4. Bond distance, average bond distance, and difference of calculated bond distance from the experiment. All the values reported here are in Å.

Bond	Experiment (E)	Calculated (C)					
		B3LYP LANL2DZ(Re)6-311++G(d,p)	B3PW91 SDDALL(Re)6-31G(d,p)	PBE0 SDDALL(Re)6-31G(d,p)	MO6L SDDALL(Re) 6-31G(d,p)	MO6L LANL2DZ(Re) 6-311++G(d,p)	B3LYP SDD(Re) 6-311G*
Re1-O4	2.13	2.15	2.13	2.14	2.16	2.15	2.16
Re1-N3	2.23	2.23	2.22	2.23	2.27	2.28	2.28
Re1-N4	2.17	2.20	2.18	2.19	2.22	2.22	2.23
Re1-C23	1.92	1.92	1.92	1.93	1.91	1.93	1.94
Re1-C24	1.91	1.91	1.92	1.92	1.91	1.92	1.93
Re1-C22	1.92	1.93	1.93	1.93	1.92	1.93	1.94
Average bond distance	2.05	2.06	2.05	2.06	2.07	2.07	2.08
E-C		0.01	0.00	0.01	0.02	0.03	0.02

Supporting Information for molecular docking studies

The docking studies for the metal complexes binding with various DNA models, based on binding method (Minor groove binding – 1BNA, Major groove binding – 1BWG, Covalent cross linking – 1AU5, and Intercalation – 3FT6 and 1Z3F), is carried out in AutoDock.[5] The DNA structures are acquired from Protein Data Bank.[6] Initially, the undesirable water molecules and ligands are eliminated from the structure, then polar hydrogens are added to it. The interaction of complex-DNA explored with grid box (1BNA – 60 Å ×58 Å ×94 Å, 1BWG – 48 Å ×50 Å ×90 Å, 1AU5 – 40 Å ×52 Å ×40 Å, 3FT6 – 40 Å ×40 Å ×50 Å, and 1Z3F – 48 Å ×44 Å ×52 Å) and 0.5 grid resolution. For Re-F docking with 1Z3F, grid box of 52 Å ×40 Å ×46 Å with 0.375 grid resolution is preferred to get the intercalation mode of binding. The complexes have two torsional degrees of freedom except the Re-Me complex (torsion = 1). Docking is analyzed with 500 conformers and population size of 1500. Genetic algorithm preferred with parameters such as number of generations (27,000), mutation rate (0.02) and crossover rate (0.8). Additionally, each calculation is

repeated for five times to verify the obtained results consistency towards the conformer. Finally, the best conformer is selected based on the highest binding energy and the total number of hydrogen bonds and the binding energy value is given in Table S5. Further, BIOVIA Discovery Studio Visualizer is used for visualizing the best interactive conformer to the DNA.

Table S5 Metal complexes binding energy [kcal/mol] with various DNA models

DNA	Complexes				
	Re-F	**Re-Cl**	**Re-Br**	**Re-Me**	**Re-Np**
1BNA	-8.69	-9.75	-10.21	-9.52	-10.50
1BWG	-7.55	-8.34	-8.56	-8.24	-8.78
1AU5	-6.18	-6.41	-6.69	-6.62	-6.89
3FT6	-7.80	-8.00	-8.13	-8.31	-8.56
1Z3F	-7.17	-8.30	-8.44	-8.59	-8.41

Supporting Information for molecular dynamics simulations

To carry out the molecular dynamics (MD) simulations, the force fields for the prepared complexes are required. However, the complexes are new and the force fields are not available. Hence, we parameterised the force fields for the prepared complexes. The details are provided here.

The MD simulations for the complex with 1BNA and 1Z3F is executed in Amber 2022.[7] Optimization, frequency and Merz-Kollman population analysis calculations are performed using same density function theory and basis set (B3PW91/SDDALL(Re)/6-31G(d,p)) as mentioned earlier. From the output files, the metal complex is parameterized by easyPARM.[8] For the DNA, hydrogens are added using web-server H++.[12] Then, the metal complex and DNA added together to get the topology and coordinate files using tleap with DNA.bsc1 force field.[10] TIP3P solvation model[11] induces water molecules around complex and DNA with buffer distance of 10 Å. To neutralize the system, Na^+ ions are added. First, minimization calculation is carried out in a restrained constant volume periodic boundary condition with 10,000 steps and cut off distance of 10.0 Å. The system is fixed to be in 500 kcal/mol force constant in minimization calculation. Then, the second minimization is calculated with unrestraint constant volume periodic boundary with 2500 steps with same cut off distance as previous minimization. Next, the system is heated to 300 K over the period of 20 ps in 100000 steps. Also, the DNA and metal complex is restrained with constant volume boundary condition, 10 kcal/mol force constant and similar cut off distance. The MD simulation performed for all the complex at 300 K including Langevin forces include by Langevin damping

of 1 ps^{-1}. The simulation is carried out for 100 ps, 10 ns and finally for 600 ns with 50000, 50000000, and 300000000 steps respectively. The time step is set to be 2 fs without any constraints. Trajectory is analyzed by Cpptraj (AMBER) and Visual Molecular Dynamics software is used for visualization.[12] The binding of metal complex with DNA has been assessed using MM-PBSA method in Amber.[13]

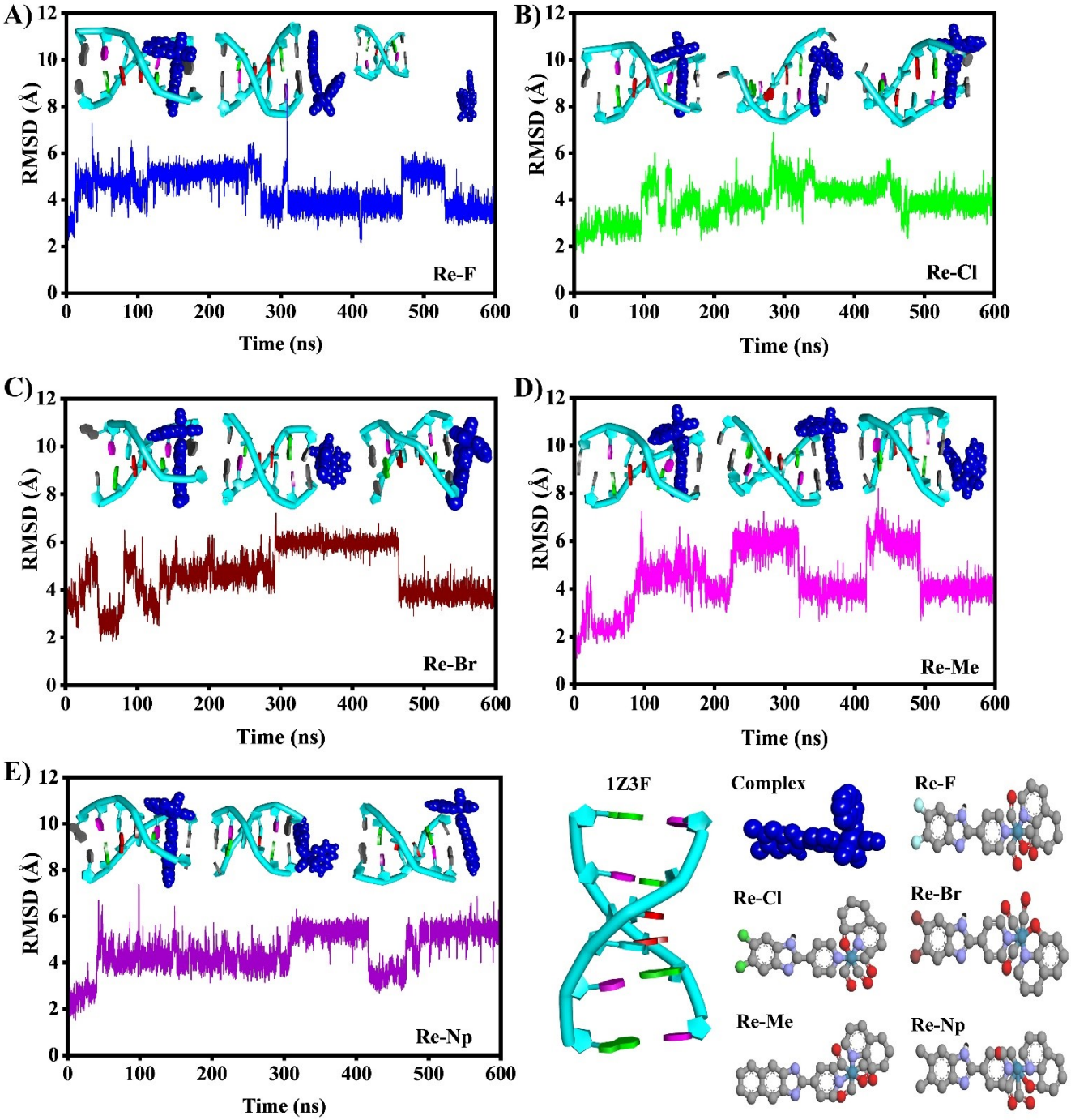

Fig. S27 Time evoluation of RMSD of metal complexes-1Z3F A) **Re-F**, B) **Re-Cl**, C) **Re-Br**, D) **Re-Me**, and E) **Re-Np**. The metal complexes are colored in blue for better visualization in the 3D representation. The inserted snapshot in the plot is taken at 0 ns, 300 ns, and 600 ns respectively. The atoms' colors are represented as follows: Grey – C, Black – H, Blue – N, Red – O, Cyan – Re, Pale blue – F, Green – Cl , and Brown – Br.

Table S6 MMPBSA calculations of **Re-F**, **Re-Cl**, **Re-Br**, **Re-Me,** and **Re-Np** with 1Z3F. All values are reported in kcal/mol.

Complexes	Re-F	Re-Cl	Re-Br	Re-Me	Re-Np
VDWAALS	–20.9	–38.3	–33.7	–35.6	–38.4
EEL	–5.4	–14.3	–8.5	–6.9	–3.7
EGB	13.4	27.6	20.8	20.8	19.0
ESURF	–1.8	–3.2	–2.7	–3.2	–3.1
ΔG (gas)	–26.3	–52.6	–42.2	–42.7	–42.0
ΔG (solv)	11.5	–24.4	18.1	17.5	15.9
ΔG (binding)	–14.8	–28.2	–24.1	–25.1	26.1

References

1. M. Priyatharsini, I. Mishra, B. Shankar, N. Srinivasan, R. V. Krishnakumar and M. Sathiyendiran, *J. Organomet. Chem.* 2021, **953**, 122052. (doi:10.1016/j.jorganchem.2021.122052)
2. G. N. Pallewela and R. P. A. Bettens, *Chem. Pap* 2023, **77**, 47–61. (doi:10.1007/s11696-022-02340-8)
3. F. Ponte, S. Scoditti, P. Barretta and G. Mazzone, *Inorg. Chem.* 2023, **62**, 8948−8959. (doi:10.1021/acs.inorgchem.3c00592)
4. J. Frisch, G. W. Trucks, H. B. Schlegel, G. E. Scuseria, M. A. Robb, J. R. Cheeseman, G. Scalmani, V. Barone, G. A. Petersson, H. Nakatsuji, X. Li, M. Caricato, A. V. Marenich, J. Bloino, B. G. Janesko, R. Gomperts, B. Mennucci, H. P. Hratchian, J. V. Ortiz, A. F. Izmaylov, J. L. Sonnenberg, D. Williams-Young, F. Ding, F. Lipparini, F. Egidi, J. Goings, B. Peng, A. Petrone, T. Henderson, D. Ranasinghe, V. G. Zakrzewski, J. Gao, N. Rega, G. Zheng, W. Liang, M. Hada, M. Ehara, K. Toyota, R. Fukuda, J. Hasegawa, M. Ishida, T. Nakajima, Y. Honda, O. Kitao, H. Nakai, T. Vreven, K. Throssell, J. A. Montgomery, Jr., J. E. Peralta, F. Ogliaro, M. J. Bearpark, J. J. Heyd, E. N. Brothers, K. N. Kudin, V. N. Staroverov, T. A. Keith, R. Kobayashi, J. Normand, K. Raghavachari, A. P. Rendell, J. C. Burant, S. S. Iyengar, J. Tomasi, M. Cossi, J. M. Millam, M. Klene, C. Adamo, R. Cammi, J. W. Ochterski, R. L. Martin, K. Morokuma, O. Farkas, J. B. Foresman, and D. J. Fox, Gaussian, Inc., Wallingford CT, 2016.
5. G. M. Morris, H. Ruth, W. Lindstrom, M. F. Sanner, R. K. Belew, D. S. Goodsell and A. J. Olson. *J Comput Chem.* 2009, **30**, 2785–91. (doi:10.1002/jcc.21256)
6. H. R. Drewt, R. M. Wingtt, T. Takanot, C. Brokat, T. Shoji, K. Itakuraii, and R. E. Dickerson. *Proc Natl Acad Sci U S A.* 1981, **78**, 2179−83 (doi:10.1073/pnas.78.4.2179)
7. D. A. Case , H. M. Aktulga , K. Belfon , D. S. Cerutti , G. A. Cisneros , V. W. D. Cruzeiro , N. Forouzesh , T. J. Giese , A. W. Götz , H. Gohlke , S. Izadi , K. Kasavajhala , M. C. Kaymak , E. King , T. Kurtzman , T.-S. Lee , P. Li , J. Liu , T. Luchko , R. Luo , M. Manathunga , M. R. Machado , H. M. Nguyen , K. A. O'Hearn , A. V. Onufriev , F. Pan , S. Pantano , R. Qi , A. Rahnamoun , A. Risheh , S. Schott-Verdugo , A. Shajan , J. Swails , J. Wang , H. Wei , X. Wu , Y. Wu , S. Zhang , S. Zhao , Q. Zhu , T. E. Cheatham, III , D. R. Roe , A. Roitberg , C.

Simmerling , D. M. York , M. C. Nagan and K. M. Merzm, Jr. , *J. Chem. Inf. Model.*, 2023, **63** , 6183–6191. (doi: 10.1021/acs.jcim.3c01153)
8. A. M. A. Abdelgawwad and A. Francés-Monerris, *J. Chem. Theory Comput.* 2025, **21**, 1817–1830. (doi: 10.1021/acs.jctc.4c01272)
9. J. C. Gordon, J. B. Myers, T. Folta, V. Shoja, L. S. Heath and A. Onufriev, *Nucleic Acids Res.* 2005, **33**, W368–W371. (doi: 10.1093/nar/gki464)
10. I. Ivani, P. Dans, A. Noy, I. Pérez, A. Faustino and A. Hospital, et al. *Nat Methods*. 2015**, 30**, 55–58. (doi: 10.1038/nmeth.3658)
11. W. L. Jorgensen, J. Chandrasekhar, J. D. Madura, R. W. Impey and M. L. Klein, *J. Chem. Phys.* 1983, **79**, 926–35. (doi: 10.1063/1.445869)
12. W. Humphrey, A. Dalke and K. Schulten. *J Mol Graph.* 1996, **14**, 33–38. (doi: 10.1016/0263-7855(96)00018-5)
13. P. A. Kollman, I. Massova, C. Reyes, B. Kuhn, S. Huo, L. Chong, et al. *Acc Chem Res.* 2000, **33**, 889–97. (doi: 10.1021/ar000033j)